Anonymous Referee #1

This is an interesting study which investigates the high tropospheric ozone values over the Mediterranean region using satellite observations and regional air quality modelling with WRF-chem. The interpretation and discussion of the results can be improved. I suggest publication of the manuscript after taking into account the following comments.

1) Introduction: They authors refer to the specific summer circulation conditions by linking to the descending branch of the Hadley cell (Bolle, 2002). Then they refer to the theory of Rodwell and Hoskins (1996) in which though (and in contrast to their previous sentence) it is proved that the subsidence center in the eastern Mediterranean is governed by Asian monsoon (and not the Hadley circulation) through the interaction of eastward propagating equatorially trapped Rossby waves (induced by the Asian monsoon heating) with mid-latitude westerlies. There are also recent studies on the influence of South Asian monsoon on summer circulation over Eastern Mediterranean (see e.g. Tyrlis et al., The summer circulation in the eastern Mediterranean and the Middle East: influence of the South Asian Monsoon, Climate Dynamics, 2013). I would suggest more thorough discussion of the dynamical processes of the summer circulation over Mediterranean.

The discussion was updated with the dynamical process of circulation and it now reads:

[…] "The dynamical processes of the summer circulation over the Mediterranean were previously attributed to the Hadley cell considered as the driver of the major subtropical dry zones. Rodwell and Hoskins (1996) argued that during the June-August period, the zonal mean Hadley circulation has very little motion and cannot explain the dry season of North Africa and the Mediterranean. Rodwell and Hoskins (1996; 2001) suggested, through numerical simulations, that the Asian monsoon heating induces an equatorially trapped Rossby wave to its west that interacts with the mid-latitude westerlies, producing a region of adiabatic descent and triggering subsidence. Long term analysis of dP/dt (units: Pa.s^{-1}, used to represent subsidence) shows indeed a positive enhancement over the Mediterranean region (Ziv et al., 2004) making the South Asian monsoon a fundamental driver of the summer circulation over the Eastern Mediterranean (Tyrlis et al., 2013)."

2) In page 12385, lines 8-9: The authors state that spring is the season known for stratosphere to troposphere exchange events. This is not absolutely true. The fact that STE maximises in late winter/early spring does not mean that is the only period that takes place (see e.g. Stohl et al., Stratosphere–troposphere exchangeâA˘Ta review, ˘ and what we have learned from STACCATO, J. Geophys. Res., 2003; Zanis et al., An estimate of the impact of Stratosphere-to-Troposphere Transport (STT) on the lower free tropospheric ozone over the Alps using 10Be and 7Be measurements J. Geophys. Res., 2003).

We agree. To avoid confusion, we updated this sentence and removed the confusing expression (also suggested by the second reviewer). The new sentence now reads:

"Increasing values in spring (MAM) are due to the increase of O_3 production from photochemistry, buildup of winter O_3 and its precursors, transport, and/or from O_3 of stratospheric origin integrating into the troposphere."

3) In Figure 6 they WRF-chem ozone values are compared with the station data. However the comparison in Figure 6 mixes the data from the different stations into one timeseries. I would suggest a more clear presentation of the model evaluation with EMEP observations for each station separately. This does not mean to add more figures for each station but maybe a Table with the evaluation scores for each individual EMEP station.

To avoid the mixing of data in Figure 6b, we removed it and instead we added as suggested a table with the correlation coefficient of each station. The table added in the manuscript is as follows:

Table 2. Pearson correlation coefficient, bias and the corresponding mean normalized bias (MNB) of each EMEP and WRF-Chem ground station data localized in Fig. 2, for the period JJA 2010.

Station name	Corr. Coef. With WRF-Chem	Bias (ppbv)	MNB (%)
CY02	**0.63**	**-7.78**	**(-14.2%)**
ES06	**0.41**	**+7.26**	**(+20.9%)**
ES07	**0.77**	**-7.24**	**(-13.4%)**
ES10	**0.72**	**+1.43**	**(+3.6%)**
ES12	**0.80**	**-5.96**	**(-12.7%)**
ES14	**0.78**	**-2.99**	**(-6.4%)**
GR02	**0.62**	**-7.38**	**(-11.3%)**
MK07	**0.57**	**-16.65**	**(-23.9%)**

4) Mind that in Figure 10 the middle troposphere IASI ozone values are higher than the respective modeled values resulting in steeper ozone gradient at upper troposphere in the modeled values. Does this mean that maybe WRF underestimates the downward transport?

The WRF-Chem data as shown in Figure 7 are smoothed with the averaging kernels of IASI. It shows that indeed the model underestimates IASI data below 10 km. This explains why in Figure 10 (also smoothed) this underestimation can be seen. This may imply that the WRF-Chem underestimates downward transport. The background O_3 values in the troposphere are not only controlled by the downward transport. The fact that the underestimation is systematic tends to indicate another reason. More detailed analysis is required (that is beyond the scope of this study) to confirm it.

5) It should be clarified that the O3-inflow tracer cannot distinguish between horizontal and vertical transport. Hence it is useful in the study the use of stratospheric tracers

Such\ as Potential Vorticity (PV) and water vapour mixing ratio to distinguish the transport from the stratosphere. The discussion though in this part is limited lacking of interpretation of the dynamical transport processes. Why it is shown in Figure 11 only the layer between 350-250 hPa and not the 4, 6 and 8 km levels for comparability reasons with Figure 9? Also mind that theoretically the water vapour mixing ratio is a better transport tracer than relative humidity (which is used in Figure 11).

We mention in P.12383 L8-10: "Since in this version of WRF-Chem the stratospheric O_3 is controlled by the lateral boundaries, O3 from stratospheric intrusions within the regional domain would be labeled as $O_{3\text{-INFLOW}}$ as well."

We agree that this should be emphasized later on too, so we add a sentence before discussing PV and the water vapor mixing ratio.

"Since stratospheric intrusions within the regional domain are included in the $O_{3\text{-INFLOW}}$ tracer, it is useful to use other stratospheric tracers to distinguish the transport from the stratosphere. PV and Q_{vap} measurements can be used as markers of transport […]"

As suggested, we replace RH with water vapor mixing ratio (Q_{vap}) measurements from the model and we also updated Figure 11 with the plots at 4, 6, and 8 and 10 km.

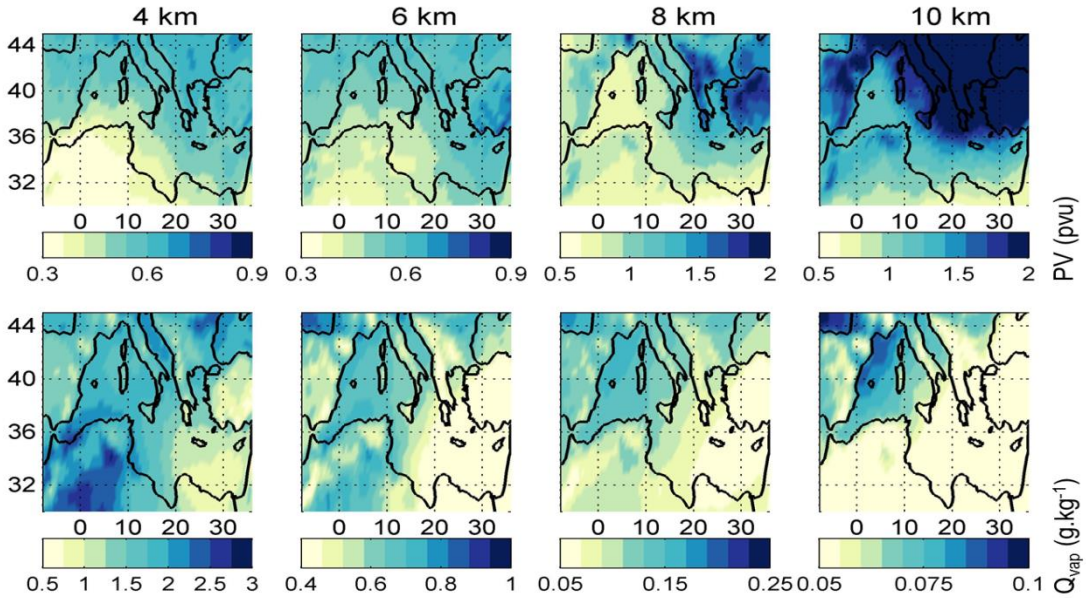

Fig. 11. WRF-Chem (a) potential vorticity (PV) at 4, 6 and 8 and 10 km over the Mediterranean region for JJA 2010. (b) Qater vapor mixing ratio (Q_{vap}) for the same vertical levels and time period.

6) The fact that the northeastern corner of the modelled domain in panels 9d-f show anthropogenic contribution between 20 and 40% needs more elaboration and justification.

We agree that the contribution of anthropogenic tracer is not negligible, and we attempt to discuss it as follows:

"The northeastern corner of the modeled domain in panels (d-f) show anthropogenic contribution between 20 and 40%. This might be due to important vertical transport and mixing in the free troposphere. These values can be correlated with the O_3 residuals plotted in panels (j-l). These panels show an O_3 signature in the north eastern corner of the domain. This signature is probably related to the emitted O_3 precursors from fires sources in the model domain (Fig. 2) and lifted to the upper troposphere due to convective movements during the Russian fires of summer 2010. We can also suppose that certain anthropogenic O_3 precursors, like NO_x, near the fire sources were also transported with the same convective movements to the same part of the domain and contributed eventually to the production of anthropogenic O_3 in that region ."

7) The section with the conclusions should be elaborated more with discussion in association with previous published studies. There are a number of published studies that have looked the high mid-tropospheric ozone values over Eastern Mediterranean.

We updated the manuscript with a new elaborated conclusion with a discussion of previous works:

"[…] Focusing on summer 2010, we use IASI and the regional chemical transport model WRF-Chem to interpret these maxima. A tagging scheme is used to keep track of O_3 from anthropogenic sources in the domain ($O_{3\text{-ANTHRO}}$) and O_3 from inflow at the domain boundaries and stratosphere ($O_{3\text{-INFLOW}}$). Our results show that transport plays an essential role in the O_3 budget over the Mediterranean troposphere and that summer O_3 maxima over the region are recorded especially in the eastern part of the basin. Even though high local anthropogenic emissions are responsible to 60-100% of O_3 in the boundary layer (surface-2 km), as demonstrated by the anthropogenic O_3 tracer of the WRF-Chem model, above 2 km, O_3 is mainly transported. Kalabokas et al. (2007, 2013) showed that the highest ozone concentrations in the low troposphere are associated with large-scale subsidence of ozone-rich air masses from the upper troposphere. However, Zanis et al., (2013) using model simulations reported, that at the low troposphere, long distance transport and local photochemical processes dominate. In the free troposphere, WRF-Chem shows that vertical and lateral transport of O_3 take place represented by the $O_{3\text{-INFLOW}}$ tracer which is responsible for 70-100% of O_3 at 4, 6 and 8 km. In the Eastern Mediterranean, Roelofs et al. (2003) showed important contributions to elevated O_3 in the middle troposphere by transport from the stratosphere. More recently, Hess and Zbinden (2013) showed that stratospheric inter-annual O_3 variability drives significantly the O_3 variability in the middle troposphere, between 30^o

and 90°N but not the overall trend which is largely affected by transport processes. The increase in O_3 seen by the model and the IASI instrument in the eastern part of the Mediterranean basin suggests that stratosphere to troposphere exchange (STE) events contribute to elevated ozone in the upper free troposphere. This is further shown in the WRF-Chem simulations that predict elevated potential vorticity (PV) and water vapor mixing ratio (Q_{vap}) over the same region. This result is in agreement with many previous studies e.g. Butkovic et al. (1990); Varotsos and Cracknell (1993); Kalabokas and Bartzis (1998); Kalabokas et al. (2000, 2007); Kouvarakis et al.(2000); Lelieveld et al.(2002); Sprenger and Wernli (2003); Papayannis et al. (2005); Gerasopoulos et al. (2006a); Akritidis et al. (2010); Zanis et al. (2013); Doche et al. (2014) that have shown the occurrence of STE events in the eastern Mediterranean region in summer. Since O_3 maxima have the potential to strongly impact regional air quality and climate (e.g. Hauglustaine and Brasseur, 2001), the present study further demonstrate the importance of quantifying and analyzing O_3 and its sources at different altitudes in the atmosphere. Quantifying long term trends and a distinction between the different sources is crucial. This should be possible with observations and model runs over longer time scales with additional tracers to identify all O_3 sources."

8) The authors may consider that there is another similar study about summer ozone over Mediterranean from IASI under discussion in ACPD (Atmos. Chem. Phys. Discuss., 14, 13021–13058, 2014).

This reference was added in the section discussion and conclusions of the manuscript.
"A complementary study by Doche et al. (2014) using IASI data at 3 km height, also showed 6 years recurrent O_3 summer maxima in July to the east of the basin."

Anonymous Referee #2

Received and published: 23 June 2014

This paper reports on the summer ozone maximum in the Mediterranean region using the thermal infrared space-borne instrument IASI and the model WRF-Chem results with additionally ground based EMEP stations. Authors investigate the 0-10km range within the 2008-2013 summer periods with a focus in 2010. They conclude on an ozone maximum, which is greater in the eastern basin (30E) than westward (15E). From WRF-Chem, they point out, the anthropogenic emissions strongly contribute to the maximum within the 0-1km altitude, whereas above 4km the transport from outside the domain is predominant. They investigate hypothesis on stratosphere to troposphere exchanges to explain the ozone enhancement in the east compared to the central basin around 15E.

The paper is well in the scope of ACP on a very interesting topic. It should be accepted if the paper is revised and improved. Material and methodology are well appropriated.

Nevertheless, text should be more accurate and justifications are sometime insufficient. Results supported by fig 10, 11 and discussions on STE in particular are not enough convincing. Revised the conclusions and do not forget to provide recommendations.

- In the paper, could you explain the reason why you investigated 2010 as an example? Is it anomalous? Is it better documented: : : In figure 1 you qualify "it is representative": : : the June-July 2010 difference at 30_E is atypical and you mention Russian forest fires in 2010. Justify more clearly and rigorously, please, that would help.

When the model was run, we chose summer 2010 as a typical summer simply because it is the year of the anthropogenic emission inventory in the model. It turned out to be atypical because it is also the summer of the Russian heat wave, which was also interesting to discuss in the paper. We agree that stating that summer is "typical" or "representative" is not very appropriate, so we removed those 2 words in the manuscript, and discuss summer 2010 in section 2.1 when we introduce the model as follows:

[…]We focus our analysis on summer 2010, which corresponds to the year of the anthropogenic emission inventory used in the model. During July-August 2010, the Russian heat wave occurred that caused severe fires with high O_3 and O_3 precursors' emissions that were probably transported to the Mediterranean region, and will be further investigated in this study."

- Could you also modify the text in order to provide the exact years used for IASI. It is specified too late in the text, only in your figure 4, 5 and conclusions.

Text was changed. We added the exact years for IASI earlier: in the abstract, the introduction and section 3.

- Description of your model should be given in the section 2.2 and not lately. The regional context of the study is unclear to me and should be improved. For example, the Figure 2 should provide : the exact model domain with the Mediterranean region you are studying (model and IASI) and you refer to in the text. Take care your text agree with the description and keep it constant. the EMEP stations you include in the study (what you did). highlight the two regions you point out is the abstract : the eastern part of the basin and the middle of the basin. Note "middle of the basin" is not specified or mentioned elsewhere in the text. The two transects provided in figure 4 are too difficult to see.

All the information about the model is now included in section 2. We thank you for the suggestion of improving figure 2. Below is an update of figure 2 with: the whole WRF-Chem domain, the region used in this study, the EMEP stations as well as the 15 and 30E transects as follows:

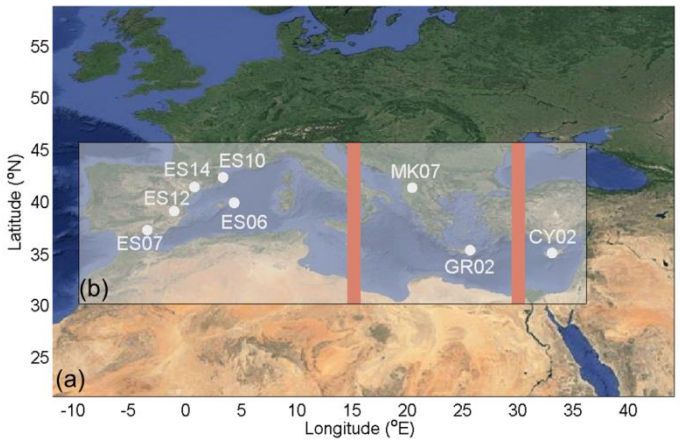

Fig 2. (a) The enlarged WRF-Chem model run domain. (b) IASI and WRF-Chem domain used in this study. White dots correspond to the location of the EMEP ground stations and the orange strips correspond to longitudinal transects at 15°E and 30°E used in Figures 5 and 10.

We add the following phrase to make clear that the transects we are choosing represent mid and east of the basin:
"we analyze longitudinal transects of 1° width along 15°E (representing the middle of the basin) and 30°E (representing the east of the basin), and marked in orange in Fig. 2."

- P12379, L2 : add "Thermal" before "infrared".

This suggestion was added to the manuscript.

- P12379, L6 : Specify exact period, "Six years (2008-2013)"…

This suggestion was added to the manuscript.

- P12380, L2 : Cairo, Istanbul and Athens you cited are located in the eastern part of the Mediterranean basin. Thus "surrounded" is not appropriated.

True. Instead of the word "basin" we now have "the eastern part of the basin"

- P12380, L7 : Would it be better to replace "region" by "circulation"???

This paragraph was elaborated, upon the suggestion of referee 1, to investigate in more detail the dynamical process from the Asian monsoon, it now reads:

[…] "The dynamical processes of the summer circulation over the Mediterranean were previously attributed to the Hadley cell considered as the driver of the major subtropical dry zones. Rodwell and Hoskins (1996) argued that during the June-August period, the zonal mean Hadley circulation has very little motion and cannot explain the dry season of North Africa and the Mediterranean. Rodwell and Hoskins (1996; 2001) suggested, through numerical simulations, that the Asian monsoon heating induces an equatorially trapped Rossby wave to its west that interacts with the mid-latitude westerlies, producing a region of adiabatic descent and triggering subsidence. Long term analysis of dP/dt (units: $Pa.s^{-1}$, used to

represent subsidence) shows indeed a positive enhancement over the Mediterranean region (Ziv et al., 2004) making the South Asian monsoon a fundamental driver of the summer circulation over the Eastern Mediterranean (Tyrlis et al., 2013).”

- P12380, L10 : The heat wave induces conditions in favour of severe fires: : : and the fires causes high O3 precursor emissions. The link between the Rossby wave and the climate extreme events with the Russian 2010 heat wave example remains in the context of your paper unclear to me…Please clarify.

This paragraph was updated; see the answer of your previous comment.

The reason why we included the Russian 2010 heat wave is just to be able to introduce it, as it is an important event that occurred in the year that we chose to model. It has an effect on the tropospheric WRF-Chem and IASI O_3 data. We separate this “link” between the Rossby wave and the Russian fires. We discuss the dynamics separately and then and we include, at a later stage, at the end of section 3, when discussing that July 2010 has the highest recorded IASI O_3 column, a note about the Russian fires.

- P12380, L12 : Could be better to replace “in Europe” by “for the European Union”.

This suggestion was added to the manuscript.

- P12381, L12 : Expression “Mediterranean atmosphere” should be more accurate, from X to X altitude or hPa, because your title is on tropospheric O3 and definition of troposphere is not given…

In this study we use the [0-8] km O_3 IASI column to assess the 2008-2013 seasonal variation. We show the averaging kernels from the surface up to 16 km. We use the [4-8] km O_3 IASI column to compare with the model, we use the WRF-Chem model at the surface, 2, 4, 6, and 8 km. and finally we show the latitude altitude plots [0-10] km for both IASI and WRF-Chem to assess stratospheric intrusions. Since we are using different combinations of columns and profiles, we choose not to be specific in the introduction, and thus we use “Mediterranean troposphere” (instead of Mediterranean atmosphere), and discuss the details in the corresponding sections.

- P12381, L24-26, the text “most of Europe” is inaccurate… Please modify the whole sentence. I expect the model domain is over Europe and the study focus on …

The sentence was changed and it now reads:
“The model domain shown in Fig. 2a is over Europe and the Mediterranean basin, the latter being the focus of this study (Fig. 2b). The horizontal resolution is of 50 km x 50 km and the vertical resolution is of 28 levels between the surface and 10 hPa.”

- It would be also interesting to specify the number of model levels relevant to the [0-10km] layer you studied.

This was included in the WRF-Chem/IASI comparison section: "the averaging kernels associated with each IASI measurement and its apriori profile are applied to the interpolated modeled profile (of around 7 layers between 4 and 10 km)"

The [0-10] km corresponds to around 19 levels (not added to the manuscript), because when we compare WRF-Chem and IASI we are using the [4-10] km column and not the [0-10] km.

- P12382, L22 : cite "Stratospheric impact on tropospheric ozone variability and trends: 1990–2009" by Hess and Zbinden, acp 2013. From this reference, you could see that the transport from lateral boundary conditions is an important term and that should be evaluated individually. As far as I understood your O3inflow include this term, Linox and STE. Please revised the text and indicate in your conclusions that to refine with more accuracy your hypothesis on STE, this evaluation would be an interesting point to investigate and solve.

The reference was added in the discussion and conclusion section (which is listed as the answer for a later comment). Indeed the $O_{3\text{-INFLOW}}$ includes transport from lateral boundaries, LiNox and STE.

- P12382, L25, "inflow" is here too imprecise, check with reference.

"inflow" was replaced with "transport".

- P12383, L12 : "Given that their contribution to the total budget in comparison with INFLOW and ANTHRO (please keep constant your labelling and modify here!) tracers is very small, they are not analysed in this study."Could you justify or at least evaluate the range of this "very small" contribution before you conclude on the O3 from fires discard from your study. Is seems to contradict to what you said P12380, line 10 on Russian fires in 2010… Note that they take place in late July and your figure 5 shows a great June-July enhancement on that specific year for the 30_E transect.

The labeling was modified to be uniform in the whole manuscript. The wording was changed since we discuss later on the residual ozone (from fires and biogenic sources) and we relate that to the Russian fires (as you also suggest in a later comment). The sentence now reads:

"Given that their contribution to the total budget in comparison with $O_{3\text{-INFLOW}}$ and $O_{3\text{-ANTHRO}}$ tracers is small (<10%), they are analyzed together in this study as "residuals" to the total budget and their contribution is defined as 100%-($O_{3\text{-ANTHRO}}$%+$O_{3\text{-INFLOW}}$%)."

- P12383, L16 : Please specify the EMEP instrumentation used.

The following sentence is added when introducing the EMEP data: "All ozone measurements within EMEP are done by UV monitors."

- P12383, L18 : In the legend the red line is not legible, adapt the colour to the red line used and your black symbol is also difficult to see. Please mention you EMEP stations are within 78m-1332m height and show up on each panel after the station name. That makes a great difference if you compare O3 at the surface with the O3 at _1000m height. It would it be interesting to show the six stations separately to improve the comparison (a table with the six stations would be convenient).

We assume that this comment is about Fig 6. We update the figure with the suggestion provided. The new figure is now as follows:

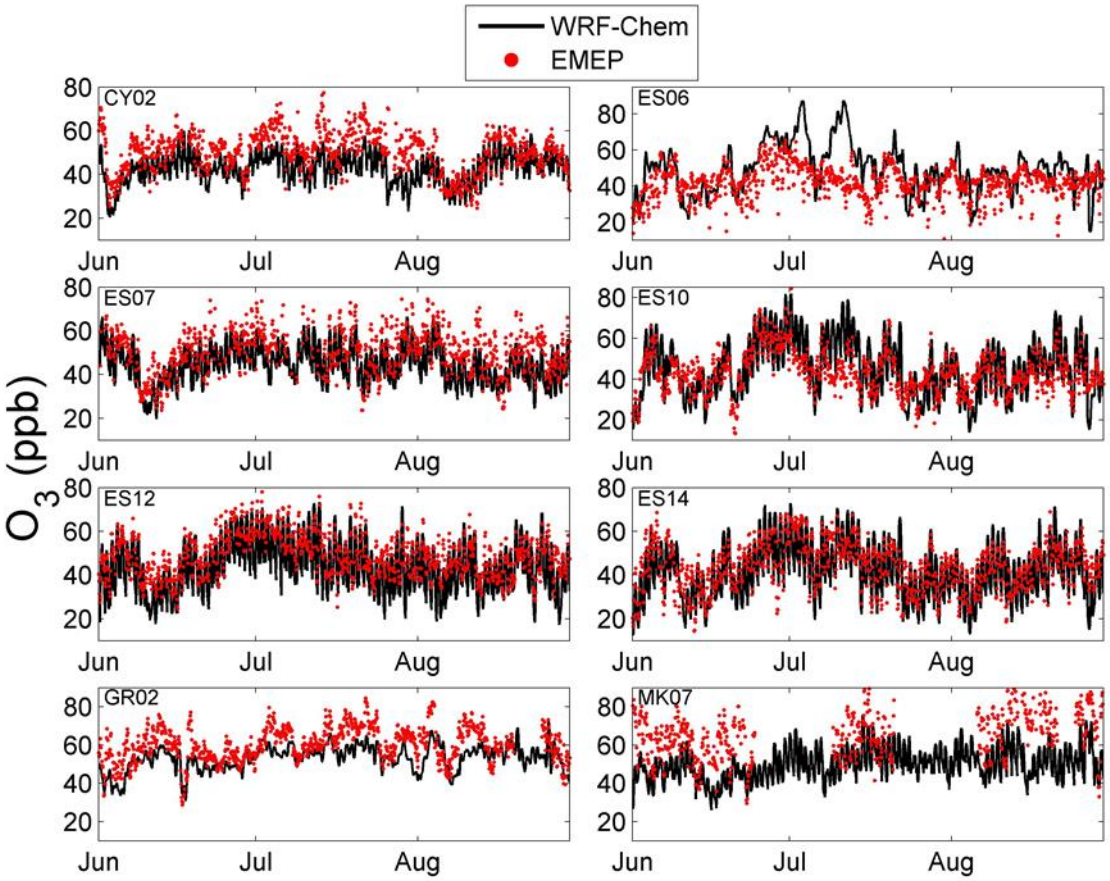

Fig. 6. O_3 time series of EMEP and WRF-Chem data at the surface for the stations localized in Fig. 2, for the period JJA 2010.

As suggested also by the first referee, we updated the manuscript with the following table. Fig 6B is therefore not necessary so we removed it. We also changed Fig 6A and the legend to make it more legible. The text was updated accordingly.

Table 2. Pearson correlation coefficient, bias and the corresponding mean normalized bias (MNB) of each EMEP and WRF-Chem ground station data localized in Fig. 2, for the period JJA 2010.

Station	Corr. Coef. With	Bias	MNB

name	WRF-Chem	(ppbv) (%)
CY02	0.63	-7.78 (-14.2%)
ES06	0.41	+7.26 (+20.9%)
ES07	0.77	-7.24 (-13.4%)
ES10	0.72	+1.43 (+3.6%)
ES12	0.80	-5.96 (-12.7%)
ES14	0.78	-2.99 (-6.4%)
GR02	0.62	-7.38 (-11.3%)
MK07	0.57	-16.65 (-23.9%)

In fact when we compare the model to the station data, we are comparing them at the same altitude, because first EMEP stations are ground based stations and the altitude recorded in Table 1 is the one above the mean sea level. Second the model takes into consideration the orography at 50 km resolution. The only discrepancy comes from the fact that the resolution of the model is coarser than reality, so if the station is located on an elevation and the surrounding is not, then the altitude taken by the model will be the one averaged of the 50x50 km around the station. Also, from the table one can see that the altitude is not really correlated with the correlation coefficient. The location of the station is a more significant factor controlling the agreement between modeled and observed O_3 concentrations.

We specified in the text that the EMEP stations are ground based stations and that the altitude in table 1 is the one above mean sea level (caption to Fig 2 and in text).

- P12384, L16 : Why do you provide the averaging kernel for the specific June 2010, your are studying the 2008-2013 period with a focus on summer 2010. Explain why.

We mention in the legend that it is a "Typical O_3 averaging kernel over the Mediterranean". We chose this one (though it is a random observation during that day) in particular during summer 2010 because it is the year we use for the model run. The justification for the choice of summer 2010 was treated in a previous comment. We change the word "Typical" to "Random" to make it more appropriate.

- P12384, L26 add partial before "tropospheric O3 column".

This suggestion is now updated in the manuscript.

- P12384, L21 "on several pollutants": which one?

The following expression was added for clarification of the pollutants measured by the IASI instruments during a case study of China pollution event: "(e.g. carbon monoxide, ammonia, sulfur dioxide and ammonium sulfate aerosols)"

- P12385, L1-2: A bit too trivial here, revise and condense using the informations on season and month from lines 5-6.

The text was changed. Line 1-2 now reads:
"The data were averaged seasonally and daytime observations were used […]"

- P12385, L9: please refer also to the "A Lagrangian "1-year climatology of (deep) crosstropopause exchange in the extratropical Northern Hemisphere" study from H. Wernli and M. Bourqui, JGR 2002 who wrote : "Generally, the cross-tropopause mass fluxes are largest in winter and smallest in summer. The most pronounced seasonal variability occurs in the southern part of the midlatitudes (30_–45_N) where the STE winter values are 2–3 times larger than the summer ones… Clarify.

Figure 7 in the suggested paper shows indeed that there are considerable STE mass fluxes in winter, but also in spring for the Med region, and much less in summer.
We agree that this part and the references are outdated and (as also suggested by the first referee) we removed this controversial sentence.

- P12385, L15-17 : Is that your definition of the eastern and middle Mediterranean region? That should have been provided before…

This was answered in a previous comment, with the description of Fig 2.

- P12385, L18-22: Should be specified that this result is a 0-8km partial O3 column and may be valuable to clarify in the introduction (P12381, L12-18) the partial layers you will investigate?

These last 2 comments were taken into consideration in the following completing sentence in the introduction:
[…] we analyze six years (2008-2013) of IASI tropospheric *[0-8] km* O_3 *column seasonal* variation above the whole Mediterranean basin *as well as at* 15^oE *and* 30^oE, *representative of what we henceforth refer as "middle of the basin" and "east of the basin" respectively*.

and we added also in P12385, L18-22 the specification that it is the [0-8] km column.

- Figure 6 (a) : I could not find the CY2 station, should it be GR02?: : : Please check and modify.

Indeed it is called CY02 but reported previously (typo) as CY01, this was corrected.

- P12386, L11 : The model underestimates… Yes, from your fig 6b. But from 6a, I have the feeling the E06 (at 78m) and ES10 (at 23m) is in better agreement with an overestimate in July for these two stations, which stations are the closest to the surface. I noticed the Stations ES07 and MK 07 are above 1km. Furthermore, your Fig 8 highlight the difference between the modelled WRF-Chem O3 concentrations at the surface and 1km. Therefore may be interesting to provide the six individual results in a table instead of Fig 6b as said

previously. A table was provided with the corresponding individual results instead of Fig 6b.

See previous comment. The stations are ground based stations and the altitude is the one above the mean sea level and same as the altitude reported in the model.

A table was also provided instead of Fig 6b.

- P12386, L14 : Suppress "which is around 0.5_ by 0.5_" as already given in the section 2.2 (and it is but in km) and just mention the ground resolution difference contribute to the discrepancy with the other possible reasons…

This expression was deleted and the phrase is updated as follows:
"The biases reported may be due to the resolution of the model resulting in a grid of around 50 km around the EMEP rural sites which may include other surface O_3 contributions."

- P12386, L18-20 : It is unclear what your correlation refer to (range and mean value). Is that for individual rural EMEP sites vs WRF-Chem??? Clarify

Yes, it is the correlation between EMEP and WRF-Chem, these correlation are now clearer as they are reported in the new Table 2. We also make this clear by stating it explicitly:
"Table 2 shows the individual O_3 correlation between WRF-Chem and the EMEP for each of the stations used in this study during JJA 2010. The model simulates the surface O_3 with a correlation ranging from 0.41 (ES06) to 0.80 (ES12) and a mean value of 0.52."

- P12387, L9-11 : As you provide on fig 7 the IASI and WRF-Chem results in DU for the 0-4 O3 partial column, why this summer mean bias is provided in ppbv? Is the difference less over land than over sea??? More comments are expected on that difference (line 7).

Thanks for your careful reading as the ppbv is a typo. It should be "DU". This was corrected in the manuscript.
We precise that the WRF-Chem model columns shown on the figure 7 are smoothed with the averaging kernel of IASI. Averaging kernels are variable, and particularly depend on surface properties. This means that when the model is smoothed with the AK then compared to IASI, the surface type (land/sea) should not matter. But this does not mean that the surface type has no influence on the O_3 comparison. There can be physical reasons, e.g. convection stronger over land surfaces, etc… However, in Fig. 7, we do not see a difference between land and sea and therefore we do not discuss this issue in the manuscript.

- P12387, L17-20 : Please clarify "We analyzed the IASI columnar total error relative to measurement for the [4–10]km integrated partial column", I do not understand what you meant here… Revised and clarify the whole lines 17-20.

This sentence was changed to make it simpler:
"We analyzed the IASI total retrieval error for the [4–10] km partial column"

As a side note: the total retrieval error contributions come from the limited vertical sensitivity (smoothing error), from the measurement noise and from uncertainties on fitted and fixed parameters (Hurtmans et al., 2012).

- P12387, L25 : Please note that your summer maximum occurs at 1km and careful take it into account in your EMEP comparison at _1km with WRF-Chem surface.

The issue of stations altitude was treated in a previous comment.

- P12388, L3 : "the entire model study …10 hPa" : this should be removed from this section and included in section 2.2. What "the entire model study" means. Keep the labelling steady or explain the difference.

This sentence was condensed and now reads: "In order to investigate possible sources of high O_3, we run the model with 2 different tracers of pollution: $O_{3\text{-ANTHRO}}$ and $O_{3\text{-INFLOW}}$ as described in section 2.1. *$O_{3\text{-ANTHRO}}$ (Fig. 8 d-f) assesses the possible anthropogenic contribution of O_3 at different altitudes, while $O_{3\text{-INFLOW}}$ (Fig. 8 g-i), provides an estimate of transport of O_3 including the stratosphere."*

The sentence : "the entire model study …10 hPa" was removed since it is already mentioned in section 2.1: "The model domain shown in Fig. 2a is over Europe and the Mediterranean basin, the latter being the focus of this study (Fig. 2b). The horizontal resolution is of 50 km x 50 km and the vertical resolution is of 28 levels between the surface and 10 hPa."

- P12388, L4 : To what I understood, these residuals plots should reveal the O3 from biogenic sources and O3 from fires… This seems in contradiction with what is said on P12383 L 12-14.

The residual plots represent the ozone from biogenic and fire sources. We make it clear by stating it twice in the text.

We change P12383 L 12-14, so it reads:
"Two more tracers are available to complete the O_3 budget: O_3 from biogenic sources and O_3 from fires. Given that their contribution to the total budget in comparison with $O_{3\text{-INFLOW}}$ and $O_{3\text{-ANTHRO}}$ tracers is small (<10%), they are analyzed together in this study as "residuals" to the total budget and their contribution is defined as 100%-($O_{3\text{-ANTHRO}}$%+$O_{3\text{-INFLOW}}$%)."

We change P12388 L4: "The residual plots plotted in panels (j-l) represent the completion of the O_3 budget, and represent the O_3 contribution from fires and biogenic sources. These plots show that the residual contribution is between 0 and 10% inferring that the $O_{3\text{-ANTHRO}}$ and $O_{3\text{-INFLOW}}$ are responsible of 90 to 100% of the total O_3 budget over the model domain, at the different altitudes of Fig. 8 and 9.

- P12388, L5 : Provide evaluation in the text instead of “most”, too imprecise.

The wording is changed, it now reads:

“These plots show that the residual contribution is between 0 and 10% inferring that the $O_{3\text{-}ANTHRO}$ and $O_{3\text{-}INFLOW}$ are responsible of 90 to 100% of the total O_3 budget over the model domain, at the different altitudes of Fig. 8 and 9.”

- P 12389, L 13-14 : the extended domain… includes the Russian fires ??? Still the same, your domain (here extended) is not rigorously defined. You must define this clearly and rigorously in section 2.

The exact model domain is now more rigorously presented in Figure 2 and also discussed in section 2.

- Figure 10 : Replace “along” which is confusing by “at” and add after “15_ E” “(left)” and “30_ E” “(right)”. Remove from the figure caption : “The Eastern part of the basin : : :events” Could you add in the text or figure the altitude of your seasonally-averaged coldpoint, quartiles tropopause or the dynamical tropopause at 2pvu with statistics on the quartiles to be more meaningful: : : I have the feeling your 100ppbv is more above 8km than between 6-8km (also on fig 9c).

The suggestions for the caption were implemented. We also added on the plot the dynamical tropopause height.

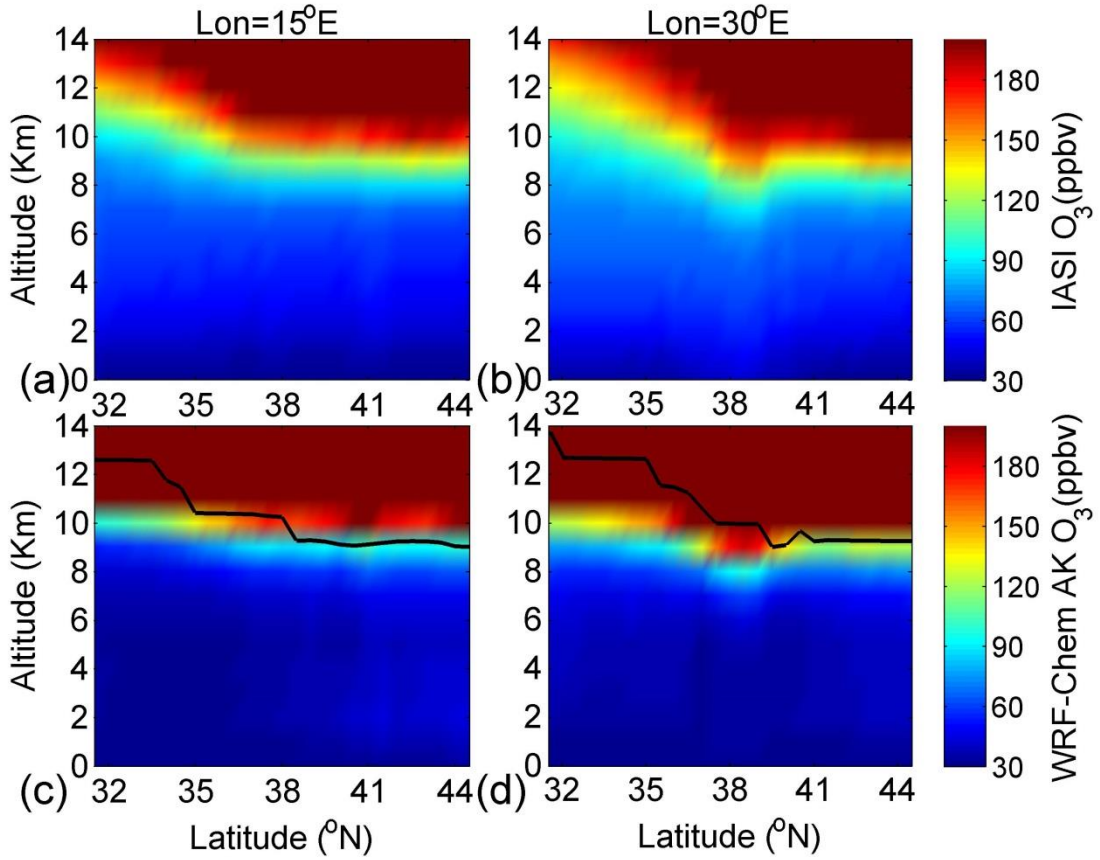

Fig.10. Mean latitude-altitude cross sections of IASI-O_3 (a-b) and modeled-O_3 (c-d) averaged over JJA 2010 at 15°E (left) and 30°E (right). Black line corresponds to the dynamical tropopause height.

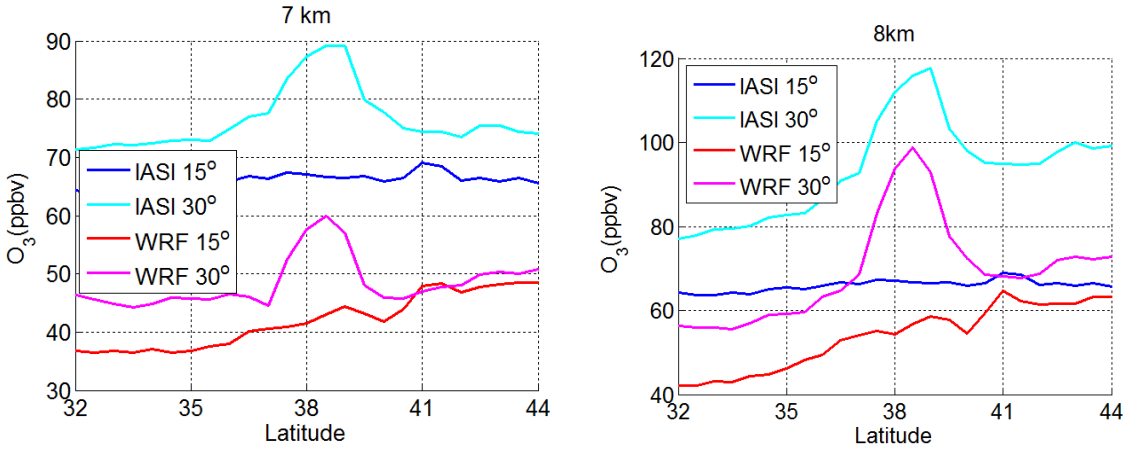

Fig_A: O_3 from IASI and WRF-Chem (smoothed with the IASI AK) at 7 and 8 km.

Fig_A shows that at 8 km values of 100 ppbv are reached for IASI and WRF-Chem at around 38.5 E.

- Undoubtedly you have more ozone at 30_E than at 15_E. Nevertheless, I am not convinced by your concluding remark because below 8km I can't see any typical STE features as described in the figure 5a and 5 from Zanis et al. 2014 showing O3 values much higher that 100ppbv in July-August within 1998-2009. Moreover your 2010 JJA-average include a June low O3 anomaly at 30_E. The highest PV values you cite 0.8 to 1.4 pvu in the east-basin and the lowest are 0.6-0.9 in the midbasin (15_E) appears as typical tropospheric PV values. STE events should provide higher values, is that the effect of the 3-month averaging?: : : To me the June 2010 doesn't seem to be so typical and probably lessen you result in 10 b and 10 c. Your O3inflow is not an exclusive tracer on O3 from STE and you mentioned from Pfister al al (2013) the transported plumes over large distance might not be well resolved from the model. To improve may be valuable to provide if possible where, when and how frequent the maximum PV-values are occurring in your model after the tropopause position has been clarified. STE events are not shown so clearly on fig 10 at least it could be transients or shallow events. I recommend concluding more carefully on the impact of STE and using "suggest" which seems to me more appropriated. Figure 11 and Page 12289 L 21 : Provide the longitudes in Fig 11a-b. After the figure 10, this figure doesn't help much to conclude on STE. The layer you investigate is _8-10km whilst the fig 10 is within 0-10km

This is how Fig. 10 looks like without the month June. One can note that there is little difference between this plot and the plot we had in our paper, inferring that the month of June does not change much the overall shape of Fig. 10

We also updated Fig 11 with the potential vorticity and water vapor mixing ratio at different altitudes, which makes it clearer to see that in particular at 8 and 10km we have higher PV values to the east. We discuss the results and compare it to other studies. The conclusion was changed and updated with a discussion with previous studies. We use the word "suggest" for STE.

The updated part of the conclusion now reads:

"[…] Focusing on summer 2010, we use IASI and the regional chemical transport model WRF-Chem to interpret these maxima. A tagging scheme is used to keep track of O_3 from anthropogenic sources in the domain ($O_{3\text{-ANTHRO}}$) and O_3 from inflow at the domain boundaries and stratosphere ($O_{3\text{-INFLOW}}$). Our results show that transport plays an essential role in the O_3 budget over the Mediterranean troposphere and that summer O_3 maxima over the region are recorded especially in the eastern part of the basin. Even though high local anthropogenic emissions are responsible to 60-100% of O_3 in the boundary layer (surface-2 km), as demonstrated by the anthropogenic O_3 tracer of the WRF-Chem model, above 2 km, O_3 is mainly transported. Kalabokas et al. (2007, 2013) showed that the highest ozone concentrations in the low troposphere are associated with large-scale subsidence of ozone-rich air masses from the upper troposphere. However, Zanis et al., (2013) using model simulations reported, that at the low troposphere, long distance transport and local photochemical processes dominate. In the free troposphere, WRF-Chem shows that vertical

and lateral transport of O_3 take place represented by the $O_{3\text{-INFLOW}}$ tracer which is responsible for 70-100% of O_3 at 4, 6 and 8 km. In the Eastern Mediterranean, Roelofs et al. (2003) showed important contributions to elevated O_3 in the middle troposphere by transport from the stratosphere. More recently, Hess and Zbinden (2013) showed that stratospheric inter-annual O_3 variability drives significantly the O_3 variability in the middle troposphere, between 30° and 90°N but not the overall trend which is largely affected by transport processes. The increase in O_3 seen by the model and the IASI instrument in the eastern part of the Mediterranean basin suggests that stratosphere to troposphere exchange (STE) events contribute to elevated ozone in the upper free troposphere. This is further shown in the WRF-Chem simulations that predict elevated potential vorticity (PV) and water vapor mixing ratio (Q_{vap}) over the same region. This result is in agreement with many previous studies e.g. Butkovic et al. (1990); Varotsos and Cracknell (1993); Kalabokas and Bartzis (1998); Kalabokas et al. (2000, 2007); Kouvarakis et al.(2000); Lelieveld et al.(2002); Sprenger and Wernli (2003); Papayannis et al. (2005); Gerasopoulos et al. (2006a); Akritidis et al. (2010); Zanis et al. (2013); Doche et al. (2014) that have shown the occurrence of STE events in the eastern Mediterranean region in summer. Since O_3 maxima have the potential to strongly impact regional air quality and climate (e.g. Hauglustaine and Brasseur, 2001), the present study further demonstrate the importance of quantifying and analyzing O_3 and its sources at different altitudes in the atmosphere. Quantifying long term trends and a distinction between the different sources is crucial. This should be possible with observations and model runs over longer time scales with additional tracers to identify all O_3 sources."

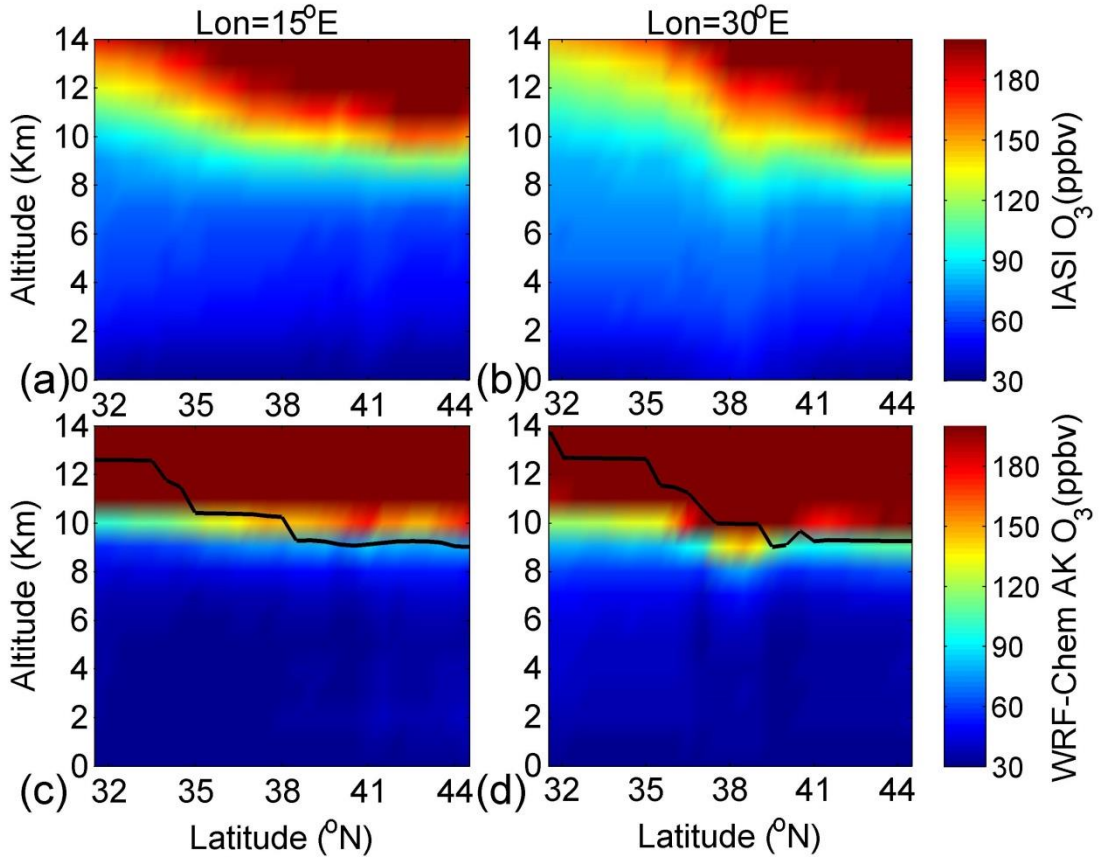

Fig_B. Mean latitude-altitude cross sections of IASI-O_3 (a-b) and modeled-O_3 (c-d) averaged over July and August 2010 at 15°E (left) and 30°E (right). Black line corresponds to the dynamical tropopause height.

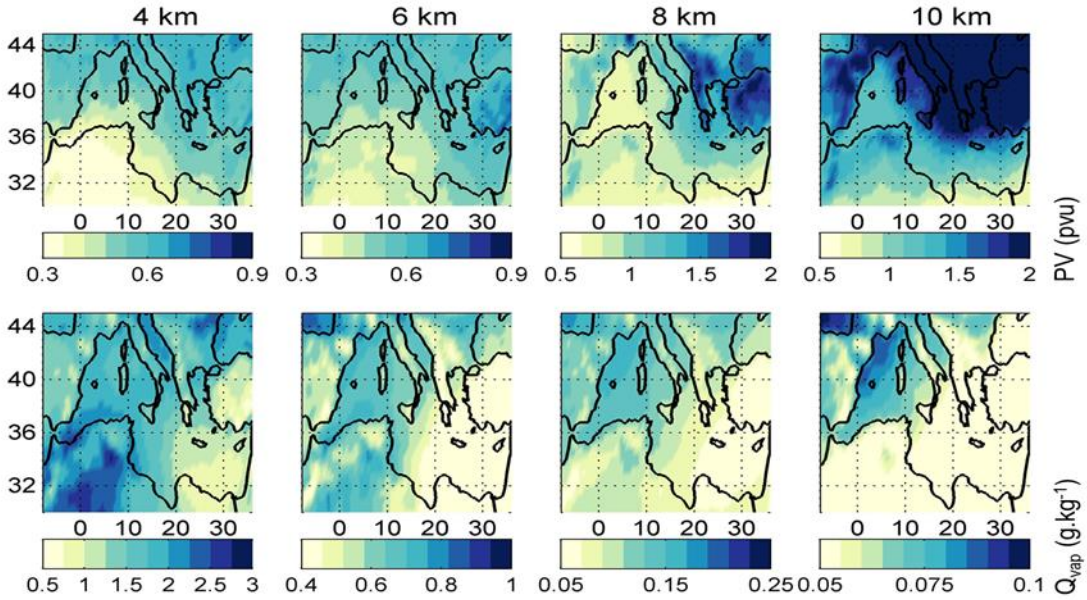

Fig. 11. WRF-Chem (a) potential vorticity at 4, 6 and 8 and 10 km over the Mediterranean region for JJA 2010 and (b) water vapor mixing ratio for the same vertical levels and time period.

References to add :

Liu et al., JGR 2011: "Influence of interannual variations in transport on summertime abundances of ozone over the Middle East".
A large number of useful references are provided by Zanis et al. 2014: : :

We added the following sentence with the reference in the introduction: " Liu et al., (2011) showed with long term model analysis that the dominant sources of O_3 in the Middle East (including the Mediterranean) are the transport from Asia and local production."
This reference and many others from Zanis et al., are now included in the manuscript, particularly in the discussion and conclusions section (see previous comment).

Take into account and refer to a study submitted recently to acpd by Doche et al, 2014 on "Summertime tropospheric ozone variability over the Mediterranean basin observed with IASI"

This reference was added in the discussion and conclusions:

"A complementary study by Doche et al. (2014) using IASI data at 3 km height, also showed 6 years recurrent O_3 summer maxima in July to the east of the basin."

Summertime tropospheric ozone assessment over the Mediterranean region using the thermal infrared IASI/MetOp sounder and the WRF-Chem model

S. Safieddine[1], A. Boynard[1], P.-F. Coheur[2], D. Hurtmans[2], G. Pfister[3], B. Quennehen[1], J. L. Thomas[1], J.-C. Raut[1], K. S. Law[1], Z. Klimont[4], J. Hadji-Lazaro[1], M. George[1] and C. Clerbaux[1,2]

[1]Sorbonne Universités, UPMC Univ. Paris 06; Université Versailles St-Quentin; CNRS/INSU, LATMOS-IPSL, Paris, France

[2]Spectroscopie de l'Atmosphère, Chimie Quantique et Photophysique, Université Libre de Bruxelles (U.L.B.), Brussels, Belgium

[3]Atmospheric Chemistry Division, National Center for Atmospheric Research, Boulder, Colorado, USA

[4]International Institute for Applied Systems Analysis, Laxenburg A-2361, Austria

Abstract

Over the Mediterranean region, elevated tropospheric ozone (O_3) values are recorded, especially in summer. We use the thermal Infrared Atmospheric Sounding Interferometer (IASI) and the Weather Research and Forecasting Model with Chemistry (WRF-Chem) to understand and interpret the factors and emission sources responsible for the high O_3 concentrations observed in the Mediterranean troposphere. Six years (2008-2013) of IASI data have been analyzed and show consistent maxima during summer, with an increase of up to 22% in the [0-8] km O_3 column in the eastern part of the basin compared to the middle of the basin. We focus on summer 2010 to investigate the processes that contribute to these summer maxima. Using two modeled O_3 tracers (inflow to the model domain and local anthropogenic emissions), we show that between the surface and 2 km, O_3 is mostly formed from anthropogenic emissions and above 4 km, is mostly transported from outside the domain or from stratospheric origins. Evidence of stratosphere to troposphere exchanges (STE) in the eastern part of the basin is shown, and corresponds with low water vapor mixing ratio and high potential vorticity.

1 Introduction

Tropospheric ozone (O_3) is a greenhouse gas, air pollutant, and a primary source of the hydroxyl radical OH, the most important oxidant in the atmosphere (Chameides and Walker, 1973; Crutzen, 1973). Previous observations and studies have shown that tropospheric O_3 over the Mediterranean exhibits a significant increase during summer time, especially in the east of the basin (Kouvarakis et al., 2000; Im et al., 2011; Gerasopoulos et al., 2005, 2006a; Richards et al., 2013; Zanis et al., 2014). Meteorological conditions such as frequent clear sky conditions (Fig. 1a) and high exposure to solar radiation (Fig. 1b) in summer enhance the formation of

730 photochemical O_3 due to the availability of its precursors. These precursors include carbon
731 monoxide (CO), peroxyl radicals generated by the photochemical oxidation of volatile organic
732 compounds (VOCs) and nitrogen oxides (NO_x = NO + NO_2). Locally, the eastern part of the
733 basin is surrounded with megacities such as Cairo, Istanbul, and Athens that are large sources of
734 local anthropogenic emissions. The geographic location of the basin makes it a receptor for
735 anthropogenic pollution from Europe both in the boundary layer (Fig. 1c) and the mid-
736 troposphere (Fig. 1d). The threshold O_3 value for air quality standards for the European Union (of
737 daily maximum of running 8-hour mean values of 60 ppbv) is exceeded on more than 25 days per
738 year at a large number of stations across Europe, many of which are located to the south of
739 Europe in the Mediterranean basin (EEA, 2012). The dynamical processes of the summer
740 circulation over the Mediterranean were previously attributed to the Hadley cell considered as the
741 driver of the major subtropical dry zones. Rodwell and Hoskins (1996) argued that during the
742 June-August period, the zonal mean Hadley circulation has very little motion and cannot explain
743 the dry season of North Africa and the Mediterranean. Rodwell and Hoskins (1996; 2001)
744 suggested, through numerical simulations, that the Asian monsoon heating induces an
745 equatorially trapped Rossby wave to its west that interacts with the mid-latitude westerlies,
746 producing a region of adiabatic descent and triggering subsidence. Long term analysis of dP/dt
747 (units: $Pa.s^{-1}$, used to represent subsidence) shows indeed a positive enhancement over the
748 Mediterranean region (Ziv et al., 2004) making the South Asian monsoon a fundamental driver
749 of the summer circulation over the Eastern Mediterranean (Tyrlis et al., 2013). High O_3 values in
750 the Mediterranean troposphere in the literature are attributed to different sources: Lelieveld et al.
751 (2002) showed that in the upper troposphere, Asian pollution is transported from the east by the
752 monsoon across the Mediterranean tropopause into the lower stratosphere. Liu et al., (2011)
753 showed with long term model analysis that the dominant sources of O_3 in the Middle East

(including the Mediterranean) are the transport from Asia and local production. On the other hand, Gerasopoulos et al. (2005) have shown that the mechanism that controls surface O_3 seasonal variability in the eastern basin during summer is mainly the transport from Europe. Galani et al. (2003) detected with lidar measurements an increase of 10% of tropospheric O_3 between 4.5 and 6.5 km due to stratosphere to troposphere exchange events (STE). Zbinden et al. (2013) using aircraft data from MOZAIC (Measurements of OZone and water vapour by in-service AIrbus airCraft programme) over 15 years (1994–2009), showed that the tropospheric O_3 columns in the east of the Mediterranean, reached a maximum reaching 43.2 DU during June-July. This recorded maximum exceeds the maximum recorded for Beijing for the same period, for example. Model calculation using WRF-Chem (Weather Research and Forecasting model coupled with Chemistry) and EMEP (European Monitoring and Evaluation Programme) MSC-W (Meteorological Synthesizing Centre-West) models of the Eastern Mediterranean during heat waves in 2007 showed that the daily maximum near surface O_3 is mostly sensitive to anthropogenic emissions of O_3 precursors (Hodnebrog et al., 2012). Im et al. (2011) found that the near surface ozone mixing ratios increases almost linearly with temperature by 1.0±0.1 ppb O_3 per Kelvin. STE processes can affect the tropospheric O_3 budget and impact air quality if transported to the boundary layer (Fiore et al., 2002). Stratospheric intrusions have been detected in the Mediterranean region, especially to the east side (Galani et al., 2003; Zanis et al., 2014), because it lies to the south of the North Hemisphere polar jet flowing over mid-latitudes (Stohl et al., 2000; Gerasopoulos et al., 2001). Understanding the factors that contribute to the O_3 maxima is important for developing control measures and prevents pollution build up. In this study we analyze O_3 and its sources at different altitudes in the Mediterranean troposphere. Section 2 introduces the model and observations data sets used in this study. In section 3, we analyze six years (2008-2013) of IASI tropospheric [0-8] km O_3 column seasonal variation above the whole

778 Mediterranean basin as well as at 15°E and 30°E, representative of what we henceforth refer as
779 "middle of the basin" and "east of the basin" respectively. In section 4 we focus on summer
780 2010, as an example year, and validate the WRF-Chem model simulation with surface O_3 and
781 IASI data, and then use the WRF-Chem model to assess the sources of O_3 in the troposphere. In
782 section 5, we use IASI and WRF-Chem free tropospheric O_3 data to investigate potential
783 stratosphere to troposphere exchange events. Discussion and conclusions are given in section 6.
784

785 **2 Model and observational data**

786 **2.1 WRF-Chem model**

787 In this study, we use the regional chemistry transport model WRF-Chem, Version 3.2 (Grell et
788 al., 2005) to assess the O_3 budget and spatio-temporal variability of O_3 over the Mediterranean
789 during summer 2010. The model domain shown in Fig. 2a is over Europe and the Mediterranean
790 basin, the latter being the focus of this study (Fig. 2b). The horizontal resolution is of 50 km x 50
791 km and the vertical resolution is of 28 levels between the surface and 10 hPa. The meteorological
792 initial and boundary conditions are based on the National Centers for Environmental Prediction
793 (NCEP) Final (FNL) analyses with analysis nudging for wind, temperature, and humidity applied.
794 Fields are provided every 6 hours with 1° horizontal resolution and 27 vertical levels from the
795 surface up to 10 hPa. The chemical initial and boundary conditions, spatially and temporally
796 varying (6 hours), are constrained by global chemical transport simulations from MOZART-
797 4/GEOS-5 with 1.9° x 2.5° horizontal resolution (Emmons et al., 2010a). The WRF-Chem gas-
798 phase chemical mechanism is that from Model for Ozone and Related Chemical Tracers, version
799 4 (MOZART-4) (Emmons et al., 2010a), which is coupled to the aerosol scheme Goddard
800 Chemistry Aerosol Radiation and Transport (GOCART) model (Chin et al., 2002). The model
801 also includes anthropogenic and fire emissions that are calculated off-line. The anthropogenic

emissions used within the WRF-Chem model were developed in the frame of the ECLIPSE European project using the Greenhouse gas and Air pollution Interactions and Synergies (GAINS) model. In addition to the ECLIPSE V4.0 anthropogenic emissions, ship emissions from the RCP 6.0 scenario (Fujino et al., 2006; Hijioka et al., 2008) were used. Biomass burning emissions are obtained from the Fire Inventory from NCAR (FINN V1) (Wiedinmyer et al., 2011). Biogenic emissions are calculated online from the Model of Emissions of Gases and Aerosols from Nature (MEGAN) (Guenther et al., 2006). The WRF-Chem simulation outputs are saved every 2 hours from 1 June 2010 until 31 August 2010.

In this study, we use a tagging method for O_3 (Emmons et al., 2012), which has been applied in global models for diagnosing contributions for individual sources to O_3 (e.g. Lamarque et al., 2005; Pfister et al., 2006, 2008; Emmons et al., 2010b; Wespes et al., 2012), and in other global and regional chemical transport models (Ma et al., 2002; Hess and Zbinden, 2013). Recently, this scheme was used for the first time in the WRF-Chem model to quantify the contribution of transport on surface O_3 over California (Pfister et al., 2013). Here, we apply this scheme to keep track of the contribution of O_3 within the WRF-Chem domain. To determine O_3 sources, tagged NO_x is traced through the odd nitrogen species (e.g. PAN, HNO_3, organic nitrates) to account for NO_x recycling (Emmons et al., 2012). Two separate tracer runs were conducted with the same emissions, initial, and boundary conditions. In the first one, $O_{3\text{-ANTHRO}}$ tracer accounts for the anthropogenic regional tagged NO_x, while the second one $O_{3\text{-INFLOW}}$ tracer accounts for tagged O_3 as well as all nitrogen species at the lateral boundaries of the regional model domain. $O_{3\text{-INFLOW}}$ tracer includes O_3 and O_3 precursors from all natural (including lightning and stratospheric O_3) and anthropogenic sources outside the regional modeling domain. Within the regional modeling domain, $O_{3\text{-INFLOW}}$ undergoes transport and chemical processes, but is not produced from sources other than from reactions including the tagged species. Since in this version of WRF-Chem the

826 stratospheric O_3 is controlled by the lateral boundaries, O_3 from stratospheric intrusions within
827 the regional domain would be labeled as $O_{3\text{-INFLOW}}$ as well. More details about the tagging
828 scheme are provided in Emmons et al. (2012). Two more tracers are available to complete the O_3
829 budget: O_3 from biogenic sources and O_3 from fires. Given that their contribution to the total
830 budget in comparison with $O_{3\text{-INFLOW}}$ and $O_{3\text{-ANTHRO}}$ tracers is small (<10%), they are analyzed
831 together in this study as "residuals" to the total budget and their contribution is defined as 100%-
832 ($O_{3\text{-ANTHRO}}$%+$O_{3\text{-INFLOW}}$%). We focus our analysis on summer 2010, which corresponds to the
833 year of the anthropogenic emission inventory used in the model. During July-August 2010, the
834 Russian heat wave occurred that caused severe fires with high O_3 and O_3 precursors' emissions
835 that were probably transported to the Mediterranean region, and will be further investigated in
836 this study.

837 **2.2 EMEP data**

838 The EMEP (European Monitoring and Evaluation Programme) O_3 hourly data
839 (http://ebas.nilu.no/) are used to validate the WRF-Chem model at the surface. All ozone
840 measurements within EMEP are done by UV monitors. In this study, measurements at 8 ground
841 rural background sites during the summer of 2010 are used. Details on the EMEP observation
842 system can be found in Hjellbrekke et al. (2012). The geographic locations of the 8 stations used
843 for validation are plotted in Fig. 2 and the corresponding details are listed in Table 1. Two more
844 station data were available, GR01-Aliartos (38.37^{o}N, 23.11^{o}E) and IT01-Montelibretti (42.1^{o}N,
845 12.63^{o}E). We disregarded the data from these stations because they show strong diurnal variation
846 of 80-90 ppbv amplitude, and recurrent near zero O_3 concentrations throughout the period of the
847 study, and were thus considered unreliable.

848

849 **2.3 IASI satellite measurements**

On board of the MetOp platforms, IASI was launched in October 2006 (IASI-1) and September 2012 (IASI-2). It has been sounding operationally the atmosphere since June 2007 (IASI-1) and January 2013 (IASI-2). IASI is a nadir looking Fourier transform spectrometer that probes the Earth's atmosphere in the thermal infrared spectral range between 645 and 2760 cm^{-1}, with a spectral resolution of 0.5 cm^{-1} (apodized) and 0.25 cm^{-1} spectral sampling. Global distributions of O_3 vertical profiles are retrieved in near real time using a dedicated radiative transfer and retrieval software for the IASI O_3 product, the Fast Optimal Retrievals on Layers for IASI (FORLI-O_3) (Hurtmans et al., 2012). The IASI FORLI-O_3 observations are selected for scenes with cloud coverage below 13%, and with RMS of the spectral fit residual lower than 3.5 $x10^{-8}$ $W/cm^2.sr.cm^{-1}$. Details about the chemical components that can be measured by IASI can be found in Clerbaux et al. (2009), Coheur et al. (2009), Turquety et al. (2009), and Clarisse et al. (2011). IASI has the highest O_3 sensitivity in the mid to upper troposphere (Safieddine et al., 2013). Figure 3 shows the partial column averaging kernel function for two specific observations above land and sea during June 2010. It can be seen that the sensitivity to the O_3 profile is maximal around 4-10 km for both observations. IASI sensitivity near the surface is usually limited above the sea, as seen on the right panel of Fig. 3, and better over land as seen in the left panel, and with corresponding better thermal contrast (7.8° above land, and 1.2° above sea). In fact, IASI is able to detect several pollutants (e.g. carbon monoxide, ammonia, sulfur dioxide and ammonium sulfate aerosols), especially when large thermal contrast is combined with stable meteorological conditions leading to the accumulation of pollutants near the surface (Boynard et al., 2014).

3 Tropospheric O_3 seasonal variation as seen by IASI

To investigate the seasonal behavior of tropospheric O_3 above the Mediterranean, we plot in Fig. 4 the [0-8] km partial tropospheric O_3 column as seen by IASI, during 2008 to 2013. The data were averaged seasonally and daytime observations were used since the information content of

IASI-O_3 data is shown to be higher during the day (Clerbaux et al., 2009). We observe a similar tropospheric O_3 seasonal behavior each year. The weakest values are observed in winter (DJF) and autumn (SON), when solar activity is minimal. Increasing values in spring (MAM) are due to the increase of O_3 production from photochemistry, buildup of winter O_3 and its precursors, transport, and/or from O_3 of stratospheric origin integrating into the troposphere. The [0-8] km column reaches a maximum in summer (JJA) due to high photochemical O_3 production, horizontal transport into the region, or stratosphere to troposphere exchange, all of which will be investigated in detail in the following sections. Richards et al. (2013) detected a similar spatial distribution with the Global Ozone Monitoring Experiment-2 (GOME-2) during summers of 2007 and 2008, with values exceeding 32 DU at the east of the basin for the [0-6] km O_3 column. To investigate further the higher values detected to the east of the basin, we analyze longitudinal transects of 1° width along 15°E (representing the middle of the basin) and 30°E (representing the east of the basin), and marked in orange in Fig. 2.

Figure 5 shows that during the period of 2008 to 2013, the summers in the east of the basin, notably at 30°E (plotted in red) are marked by elevated tropospheric [0-8] km O_3 values. The difference between the two O_3 columns at the 2 different longitudes was highest (4.7 DU-22 %) during June 2012. The highest recorded values were up to 30 Dobson units (DU) in July 2010 at 30°E. This period coincides with the 2010 Russian heat wave (Schubert et al., 2011) that caused severe fires with high O_3 precursors emissions (R'Honi et al., 2013). Further discussion is provided in section 4.2

4 O_3 budget from the WRF-Chem model during summer 2010

From this section onwards, we focus our analysis on summer 2010, the year of the anthropogenic emission inventory used in the model. We evaluate the model then we discuss the O_3 budget at different altitude levels in the Mediterranean troposphere.

4.1 Model evaluation: comparison to EMEP and IASI

The model is evaluated by comparing O_3 concentrations with surface O_3 data from the EMEP stations (section 2.2), then free tropospheric O_3 data from IASI (section 2.3).

4.1.1 Comparison to EMEP surface monitoring stations

Linear spatial interpolation was applied to WRF-Chem data in order to correlate the model outputs and the EMEP data that were averaged every 2 hours to coincide with the model run output data. Figure 6 shows the individual time series of the data of the 8 stations used for the validation. Table 2 shows the individual O_3 correlation and bias between WRF-Chem and the EMEP for each of the stations used in this study during JJA 2010. The model simulates the surface O_3 with a correlation ranging from 0.41 (ES06) to 0.80 (ES12) and a mean value of 0.52. Figure 6 and Table 2 show that the model reproduces reasonably well the average amplitude of the daily cycle seen in the observation. For all stations except ES06 and ES10, the model underestimates the ground observation during the summer period with a mean normalized bias between -23.9% to -6.4%. The biases reported may be due to the resolution of the model resulting in a grid of around 50 km around the EMEP rural sites which may include other surface O_3 contributions. Other possible reasons include difficulties in simulating local flow patterns due to topography and land-sea circulation, as well as uncertainties in emissions and NO_x concentrations (Pfister et al., 2013). Our results compare well with the study by Tuccella et al. (2012) that compared WRF-Chem to 75 EMEP stations over Europe during 2007, and found that hourly O_3 exhibit a correlation with observations ranging from 0.38 to 0.83. The largest

discrepancy observed, with modeled O_3 values larger than 80 ppbv, is for the station ES06-Mahon (39.87°N, 4.32°E), which might be due a particular uncertainty in the model emissions or dry deposition over this area.

4.1.2 Comparison to IASI observations

Averaged data for summer 2010 are used for the comparison of WRF-Chem and IASI O_3 [4-10] km free tropospheric column. The modeled profile is first linearly interpolated to the time and location of the retrieval. Then, the averaging kernels associated with each IASI measurement and its *apriori* profile are applied to the interpolated modeled profile (of around 7 layers between 4 and 10 km). Figure 7 shows the spatial distribution of the [4-10] km integrated IASI and WRF-Chem model O_3 column along with the relative differences. We chose to analyze this part of the atmosphere in particular because IASI has a better sensitivity between 4 and 10 km over both land and water as shown in Fig. 3. The model reproduces well the spatial patterns seen by IASI during summer (JJA) 2010, with a correlation coefficient of about 0.93 and a summertime mean bias of 6.1 DU (25%) (not shown). The model underestimation of the [4-10] km O_3 column might due to the difficulties in resolving the high O_3 concentrations observed in transported plumes over large distances (Pfister et al., 2013). On the other hand, the high discrepancies seen over northern Africa, might be due to IASI poor spectral fits above surfaces with sharp emissivity variations particularly above the desert (Hurtmans et al., 2012), leading to a possible overestimation of the real profile. We analyzed the IASI total retrieval error for the [4–10] km partial column and we found that it is on average around 7% in the model domain, and between 7 and 12% where the discrepancies between the model and IASI are the highest.

4.2 Origins of boundary layer O_3 over the Mediterranean

Modeled O_3 concentrations are illustrated in Fig. 8 (a-c) at the surface, 1 and 2 km during JJA 2010. At the surface, modeled O_3 exhibits the highest values downwind the European continent. At 1 and 2 km the whole eastern part of the basin is characterized by high O_3 mixing ratios. In order to investigate possible sources of high O_3, we run the model with 2 different tracers of pollution: $O_{3\text{-ANTHRO}}$ and $O_{3\text{-INFLOW}}$ as described in section 2.1. $O_{3\text{-ANTHRO}}$ (Fig. 8 d-f) assesses the possible anthropogenic contribution of O_3 at different altitudes, while $O_{3\text{-INFLOW}}$ (Fig. 8 g-i), provides an estimate of transport of O_3 including the stratosphere. The residual plots plotted in panels (j-l) show the completion of the O_3 budget, and represent the O_3 contribution from fires and biogenic sources. These plots show that the residual contribution is between 0 and 10% inferring that the $O_{3\text{-ANTHRO}}$ and $O_{3\text{-INFLOW}}$ combined are responsible of 90 to 100% of the total O_3 budget over the model domain, at the different altitudes of Fig. 8 and 9. The surface shows a high contribution for the anthropogenic emission tracer ($O_{3\text{-ANTHRO}}$ > 85%), with almost zero contribution of the inflow tracer. This shows the importance of local emissions to the O_3 surface concentration. At 1 km, the highest contribution is also for the anthropogenic tracer (up to 75-80%), whereas the result is mixed at 2 km between the 2 tracers (around 50-60% for $O_{3\text{-ANTHRO}}$ and 40-50% for $O_{3\text{-INFLOW}}$), suggesting that up to 50% of the O_3 available at 2 km is being transported. The rest of the O_3 plotted in the residual plots (panels j-l) and decreasing with altitude is suggested to be from fire sources, as the extended domain (Fig 2a) used in the study includes parts of the region hit by the Russian fires of summer 2010.

4.3 Origins of free tropospheric O_3 over the Mediterranean

O_3 concentrations at 4, 6 and 8 km in Fig. 9 (a-c) show that the eastern part of the basin is subject to much higher O_3 values, reaching up to 100 ppbv between 6 and 8 km (see further discussion in section 5). The anthropogenic contribution decreases with altitude, whereas the O_3 inflow

contribution increases. The northeastern corner of the modeled domain in panels (d-f) show anthropogenic contribution between 20 and 40%. This might be due to important vertical transport and mixing in the free troposphere. These values can be correlated with the O_3 residuals plotted in panels (j-l). These panels show an O_3 signature in the north eastern corner of the domain. This signature is probably related to the emitted O_3 precursors from fires sources in the model domain (Fig. 2) and lifted to the upper troposphere due to convective movements during the Russian fires of summer 2010. We can also suppose that certain anthropogenic O_3 precursors, like NO_x, near the fire sources were also transported with the same convective movements to the same part of the domain and contributed eventually to the production of anthropogenic O_3 in that region. Panels (g-i) show that 70 to 100% of the available O_3 between 4 and 8 km does not come from local sources. The high values are likely due to long-range transport of pollution from outside the study region or transport of air masses from the stratosphere that we will discuss in the following section. The low values recorded in the residual plots in panels (j-l) show that the O_3 budget in the free troposphere over this region is controlled almost exclusively by local anthropogenic sources and transport.

5 WRF-Chem and IASI detection of stratosphere-troposphere exchange events

Figures 4, 5 and Fig. 9 (a-c) showed that the eastern part of the Mediterranean basin in summer is subject to high O_3 mixing ratios at 4, 6 and 8 km. In order to further investigate the sources and processes responsible for these enhancements, modeled and observed IASI O_3 vertical profiles in the troposphere were examined, during summer 2010, to try to detect possible stratosphere to troposphere exchange (STE) events.

Figure 10 shows the tropospheric O_3 vertical distributions along 15°E (mid-Mediterranean) and 30°E (eastern Mediterranean) for IASI (panels a and b) and WRF-Chem, smoothed with the IASI

992 averaging kernels (panels c and d) for JJA 2010. Between 4 and 8 km, panels (b) and (d) show
993 higher values of O_3 in the eastern part of the basin (30°E) with concentrations ranging between 50
994 and 100 ppbv for IASI and 40 to 100 ppbv for WRF-Chem (WRF-Chem underestimates IASI as
995 shown in Fig. 7).
996 Since stratospheric intrusions within the regional domain are included in the $O_{3\text{-INFLOW}}$ tracer, it is
997 useful to use other stratospheric tracers to distinguish the transport from the stratosphere. The
998 potential vorticity (PV) and the water vapor mixing ratio (Q_{vap}) measurements can be used as
999 markers of transport from the upper troposphere-lower stratosphere (UTLS) to the troposphere:
1000 elevated O_3 and PV, and low Q_{vap} values, would indicate that high free troposphere values are
1001 due to downward transport from the UTLS (Holton et al., 1995). Here, we study PV and Q_{vap} at
1002 4, 6, and 8 and 10 km calculated from the WRF-Chem model run parameters. Figure 11 shows
1003 that starting 4 km, higher PV and lower Q_{vap} values start to develop to the east of the basin. At 8
1004 and 10 km, the highest PV values (1.5 to 2 pvu) (potential vorticity unit, 1pvu =10^{-6} m^2 K kg^{-1} s^{-1}),
1005 and the lowest Q_{vap} values (0-0.10 $g.kg^{-1}$) are recorded to the east of the basin, in comparison
1006 with low PV values in the mid and to the west of the basin (0.5-1), with high Q_{vap} values (0.1-
1007 0.15). The high PV/low Q_{vap} values to the east are in accordance with Fig. 9 and 10, strongly
1008 suggesting that this part of the basin is subject to transport from the UTLS into the free
1009 troposphere. In fact, at 30°E and around 37°N-39°N (panels b and d of Fig. 10) both IASI and the
1010 model suggest a stratospheric intrusion. It corresponds to PV values between 1.4 and 2 pvu at 8
1011 km and Q_{vap} values around 0.05 $g.kg^{-1}$. In a recent study, Zanis et al. (2014) using 12 year
1012 climatology (1998-2009) of the ERA-interim reanalysis, also detected frequent events of STE
1013 with PV ranging between 0.4 and 1.4 pvu and specific humidity values between 0.01 and 2 $g.kg^{-1}$
1014 between 700 and 250 hPa during July and August to the east of the basin, in accordance with our
1015 results for summer 2010 at 4, 6 and 8 km.

6 Discussion and conclusions

Six years of tropospheric O_3 observations provided by the IASI mission above the Mediterranean are shown. Tropospheric [0-8] km O_3 columns shows a consistent seasonal behavior over the period 2008-2013 with pronounced maxima in summer with higher values to the east of the basin. A complementary study by Doche et al. (2014) using IASI data at 3 km height, also showed 6 years recurrent O_3 summer maxima in July to the east of the basin. Since IASI has a lower sensitivity in the lower troposphere and above the sea, anthropogenic emission contribution to the boundary layer O_3 is not well captured by the instrument. However, IASI is able to detect in the free to upper troposphere, where its sensitivity is the highest, high tropospheric O_3 values to the east of the basin during the 6 years. Focusing on summer 2010, we use IASI and the regional chemical transport model WRF-Chem to interpret these maxima. A tagging scheme is used to keep track of O_3 from anthropogenic sources in the domain ($O_{3\text{-ANTHRO}}$) and O_3 from inflow at the domain boundaries and stratosphere ($O_{3\text{-INFLOW}}$). Our results show that transport plays an essential role in the O_3 budget over the Mediterranean troposphere and that summer O_3 maxima over the region are recorded especially in the eastern part of the basin. Even though high local anthropogenic emissions are responsible to 60-100% of O_3 in the boundary layer (surface-2 km), as demonstrated by the anthropogenic O_3 tracer of the WRF-Chem model, above 2 km, O_3 is mainly transported. Kalabokas et al. (2007, 2013) showed that the highest ozone concentrations in the low troposphere are associated with large-scale subsidence of ozone-rich air masses from the upper troposphere. However, Zanis et al., (2013) using model simulations reported, that at the low troposphere, long distance transport and local photochemical processes dominate. In the free troposphere, WRF-Chem shows that vertical and lateral transport of O_3 take place represented by the $O_{3\text{-INFLOW}}$ tracer which is responsible for 70-100% of O_3 at 4, 6 and 8 km. In the Eastern

Mediterranean, Roelofs et al. (2003) showed important contributions to elevated O_3 in the middle troposphere by transport from the stratosphere. More recently, Hess and Zbinden (2013) showed that stratospheric inter-annual O_3 variability drives significantly the O_3 variability in the middle troposphere, between 30° and 90°N but not the overall trend which is largely affected by transport processes. The increase in O_3 seen by the model and the IASI instrument in the eastern part of the Mediterranean basin suggests that stratosphere to troposphere exchange (STE) events contribute to elevated ozone in the upper free troposphere. This is further shown in the WRF-Chem simulations that predict elevated potential vorticity (PV) and water vapor mixing ratio (Q_{vap}) over the same region. This result is in agreement with many previous studies e.g. Butkovic et al. (1990); Varotsos and Cracknell (1993); Kalabokas and Bartzis (1998); Kalabokas et al. (2000, 2007); Kouvarakis et al.(2000); Lelieveld et al.(2002); Sprenger and Wernli (2003); Papayannis et al. (2005); Gerasopoulos et al. (2006b); Akritidis et al. (2010); Zanis et al. (2013); Doche et al. (2014) that have shown the occurrence of STE events in the eastern Mediterranean region in summer. Since O_3 maxima have the potential to strongly impact regional air quality and climate (e.g. Hauglustaine and Brasseur, 2001), the present study further demonstrate the importance of quantifying and analyzing O_3 and its sources at different altitudes in the atmosphere. Quantifying long term trends and a distinction between the different sources is crucial. This should be possible with observations and model runs over longer time scales with additional tracers to identify all O_3 sources.

Acknowledgments. IASI is a joint mission of EUMETSAT and the Centre National d'Etudes Spatiales (CNES, France). The IASI L1 data are distributed in near real time by EUMETSAT through the EumetCast system distribution. The authors acknowledge the French Ether atmospheric database (www.pole-ether.fr) for providing the IASI L1C data and L2 temperature

data. This work was undertaken under the auspices of the O3M-SAF project of the EUMETSAT and supported by the European Space Agency (ozone CCI project). The French scientists are grateful to CNES and Centre National de la Recherche Scientifique (CNRS) for financial support. The research in Belgium is funded by the Belgian State Federal Office for Scientific, Technical and Cultural Affairs and the European Space Agency (ESA Prodex arrangement). P.F. Coheur is Senior Research Associate with F.R.S-FNRS. Support is also acknowledged from the EU FP7 ECLIPSE (Evaluating the Climate and Air Quality Impacts of Short-Lived Pollutants) project (no. 282688).

References

Akritidis, D., Zanis, P., Pytharoulis, I., Mavrakis, A., and Karacostas,T.: A deep stratospheric intrusion event down to the earth's surface of the megacity of Athens, Meteorol. Atmos. Phys., 109, 9–18, doi:10.1007/s00703-010-0096-6, 2010.

Bolle, H.-J. Ed., Mediterranean Climate: Variability and Trends, Springer-Verlag, Berlin, 2002.

Boynard, A., Clerbaux, C., Clarisse, L., Safieddine, S., Pommier M., Van Damme, M., Bauduin, S., Oudot, C., Hadji-Lazaro, J., Hurtmans, D., Coheur, P.-F.: First simultaneous space measurements of atmospheric pollutants in the boundary layer from IASI: a case study in the North China Plain, Geophys. Res. Lett., 41, 645–651 doi:10.1002/2013GL058333, 2014.

Butkovic, V., Cvitas, T., and Klasinc, L.: Photochemical ozone in the Mediterranean, Sci. Total Environ., 99, 145–151, doi:10.1016/0048-9697(90)90219-k, 1990.

Chameides, W. and Walker, J. C. G.: A photochemical theory of tropospheric ozone, J. Geophys. Res., 78, 8751–8760, 1973.

Chin, M., Ginoux, P., Kinne, S., Torres, O., Holben, B. N., Duncan, B. N., Martin, R. V., Logan, J. A., Higurashi, A., and Nakajima, T.: Tropospheric aerosol optical thickness from the GOCART model and comparisons with satellite and Sun photometer measurements, J. Atmos. Sci., 59, 461–483, 2002.

Clarisse, L., R'Honi, Y., Coheur, P.-F., Hurtmans, D., and Clerbaux, C.: Thermal infrared nadir observations of 24 atmospheric gases, Geophys. Res. Lett., 38, L10802, doi:10.1029/2011GL047271, 2011.

Clerbaux, C., Boynard, A., Clarisse, L., George, M., Hadji-Lazaro, J., Herbin, H., Hurtmans, D., Pommier, M., Razavi, A., Turquety, S., Wespes, C., and Coheur, P.-F.: Monitoring of atmospheric composition using the thermal infrared IASI/MetOp sounder, Atmos. Chem. Phys., 9, 6041-6054, doi:10.5194/acp-9-6041-2009, 2009.

Coheur, P.-F., Clarisse, L., Turquety, S., Hurtmans, D., and Clerbaux, C.: IASI measurements of reactive trace species in biomass burning plumes, Atmos. Chem. Phys., 9, 5655–5667, http://www.atmos-chem-phys.net/9/5655/2009/, 2009.

Crutzen, P. J.: A discussion of the chemistry of some minor constituents in the stratosphere and troposphere, Pure Appl. Geophys., 106-108, 1385, 1973.

Doche, C., Dufour, G., Foret, G., Eremenko, M., Cuesta, J., Beekmann, M., and Kalabokas, P.: Summertime tropospheric ozone variability over the Mediterranean basin observed with IASI, Atmos. Chem. Phys. Discuss., 14, 13021-13058, doi:10.5194/acpd-14-13021-2014, 2014.

EEA: Air Quality in Europe – 2012 Report, European Environment Agency, ISBN 978-92-9213-328-3, Luxembourg, Office for Official Publications of the European Union, doi:10.2800/55823, 2012.

Emmons, L. K., Walters, S., Hess, P. G., Lamarque, J.-F., Pfister, G. G., Fillmore, D., Granier, C., Guenther, A., Kinnison, D., Laepple, T., Orlando, J., Tie, X., Tyndall, G., Wiedinmyer, C., Baughcum, S. L., and Kloster, S.: Description and evaluation of the Model for Ozone and Related Chemical Tracers, version 4 (MOZART-4), Geosci. Model Dev., 3, 43-67, 2010a.

Emmons, L. K., Apel, E. C., Lamarque, J.-F., Hess, P. G., Avery, M., Blake, D., Brune, W., Campos, T., Crawford, J., DeCarlo, P. F., Hall, S., Heikes, B., Holloway, J., Jimenez, J. L., Knapp, D. J., Kok, G., Mena-Carrasco, M., Olson, J., O'Sullivan, D., Sachse, G., Walega, J., Weibring, P., Weinheimer, A., and Wiedinmyer, C.: Impact of Mexico City emissions on regional air quality from MOZART-4 simulations, Atmos. Chem. Phys., 10, 6195–6212, doi:10.5194/acp-10-6195-2010, 2010b.

Emmons, L., Hess, P., Lamarque, J., and Pfister, G.: Tagged ozone mechanism for MOZART-4, CAM-chem and other chemical transport models, Geosci. Model Dev., 5(6), 1531–1542, doi:10.5194/gmd-5-1531-2012, 2012.

Fiore, A. M., Jacob, D. J., Bey, I., Yantosca, R. M., Field, B. D., Fusco, A. C., and Wilkinson, J. G.: Background ozone over the United States in summer: Origin, trend, and contribution to pollution episodes, J. Geophys. Res., 107(D15), 4275, doi:10.1029/2001JD000982, 2002.

Fujino, J., Nair, R., Kainuma, M., Masui, T., and Matsuoka, Y.: Multi-gas mitigation analysis on stabilization scenarios using AIM global model, multigas mitigation and climate policy, Energ. J., 27, 343–353, 2006.

Galani, E., Balis, D., Zanis, P., Zerefos, C., Papayannis, A., Wernli, H., and Gerasopoulos, E.: Observations of stratosphere-troposphere transport events over the eastern Mediterranean using a ground-based lidar system, J. Geophys. Res., 108, D128527, doi:10.1029/2002JD002596, 2003.

Gerasopoulos, E., Zanis, P., Stohl, A., Zerefos, C. S., Papastefanou, C., Ringer,W., Tobler, L., Huebener, S., Kanter, H. J., Tositti, L., and Sandrini, S.: A climatology of 7Be at four high-altitude stations at the Alps and the Northern Apennines, Atmos. Environ., 35, 6347–6360, 2001.

Gerasopoulos, E., Kouvarakis, G., Vrekoussis, M., Kanakidou, M., Mihalopoulos, N.: Ozone variability in the marine boundary layer of the Eastern Mediterranean based on 7-year observations, J. Geophys. Res., 110, D15309, doi:10.1029/2005JD005991, 2005.

Gerasopoulos, E., Kouvarakis, G., Vrekoussis, M., Donoussis, C., Mihalopoulos, N., M., Kanakidou: Photochemical ozone production in the Eastern Mediterranean. Atm. Env. 40, 3057–3069, 2006a.

Gerasopoulos, E., Zanis, P., Papastefanou, C., Zerefos, C. S., Ioannidou, A., and Wernli, H.: A complex case study of down to the surface intrusions of persistent stratospheric air over the Eastern Mediterranean, Atmos. Environ., 40, 4113–4125, 2006b.

Grell, G. A., Peckham, S. E., Schmitz, R., McKeen, S. A., Frost, G., Skamarock, W. C., and Eder, B.: Fully coupled "online" chemistry within the WRF model, Atmos. Environ., 39, 6957–6975, 2005.

Guenther, A., Karl, T., Harley, P., Wiedinmyer, C., Palmer, P. I., and Geron, C.: Estimates of global terrestrial isoprene emissions using MEGAN (Model of Emissions of Gases and Aerosols from Nature), Atmos. Chem. Phys., 6, 3181–3210, 2006. http://www.atmos-chem-phys.net/6/3181/2006/

Hess, P. G. and Zbinden, R.: Stratospheric impact on tropospheric ozone variability and trends: 1990–2009, Atmos. Chem. Phys., 13, 649–674, doi:10.5194/acp-13-649-2013, 2013.

Hijioka, Y., Matsuoka, Y., Nishimoto, H. , Matsui, M., Kanuma, M.: Global GHG emissions scenarios under GHG concentration stabilization targets, Journal of Global Environmental Engineering 13, 97-108, 2008.

Hjellbrekke, A., Solberg,S. and Fjæraa, A.M. : Ozone measurements 2010 EMEP/CCC-Report 2/2012, available at: http://www.nilu.no/projects/ccc/reports/cccr2-2012.pdf (last access: 13 May 2014), 2012.

Hodnebrog, Ø., Solberg, S., Stordal, F., Svendby, T. M., Simpson, D., Gauss, M., Hilboll, A., Pfister, G. G., Turquety, S., Richter, A., Burrows, J. P., and Denier van der Gon, H. A. C.: Impact of forest fires, biogenic emissions and high temperatures on the elevated Eastern Mediterranean ozone levels during the hot summer of 2007, Atmos. Chem. Phys., 12, 8727-8750, doi:10.5194/acp-12-8727-2012, 2012.

Hauglustaine, D. A. and Brasseur, G. P.: Evolution of tropospheric ozone under anthropogenic activities and associated radiative forcing of climate, J. Geophys. Res.-Atmos., 106, 32337–32360, doi:10.1029/2001jd900175, 2001.

Holton, J. R., Haynes, P. H., McIntyre, E. M., Douglass, A. R., Rood, R. B., and Pfister, L.: Stratosphere-troposphere exchange, Rev. Geophys., 33, 403–439, 1995.

Hurtmans D., Coheur P.-F., Wespes C., Clarisse L., Scharf O., Clerbaux C., Hadji-Lazaro J., George M., Turquety S.: FORLI radiative transfer and retrieval code for IASI, Journal of Quantitative Spectroscopy and Radiative Transfer 113, 11, 1391-1408, 2012.

Im, U., Markakis, K., Poupkou, A., Melas, D., Unal, A., Gerasopoulos, E., Daskalakis, N., Kindap, T., and Kanakidou, M.: The impact of temperature changes on summer time ozone and its precursors in the Eastern Mediterranean, Atmos. Chem. Phys., 11, 3847–3864, doi:10.5194/acp-11-3847-2011, 2011.

Kalabokas, P. D. and Bartzis, J. G.: Photochemical air pollution characteristics at the station of the NCSR-Demokritos, during the MEDCAPHOT-TRACE campaign in Athens, Greece (20 August 20 September 1994), Atmos. Environ., 32, 2123–2139, doi:10.1016/s1352-2310(97)00423-8, 1998.

Kalabokas, P. D., Viras, L. G., Bartzis, J. G., and Repapis, C. C.: Mediterranean rural ozone characteristics around the urban area of Athens, Atmos. Environ., 34, 5199–5208, doi:10.1016/s1352-2310(00)00298-3, 2000.

Kalabokas, P. D., Volz-Thomas, A., Brioude, J., Thouret, V., Cammas, J.-P., and Repapis, C. C.: Vertical ozone measurements in the troposphere over the Eastern Mediterranean and comparison with Central Europe, Atmos. Chem. Phys., 7, 3783–3790, doi:10.5194/acp-7-3783-2007, 2007.

Kalabokas, P. D., Cammas, J.-P., Thouret, V., Volz-Thomas, A., Boulanger, D., and Repapis, C. C.: Examination of the atmospheric conditions associated with high and low summer ozone levels in the lower troposphere over the eastern mediterranean, Atmos. Chem. Phys., 13, 10339–10352, doi:10.5194/acp-13-10339-2013, 2013.

Kouvarakis, G., Tsigaridis, K., Kanakidou, M., and Mihalopoulos, N.: Temporal variations of surface regional background ozone over Crete Island in the southeast Mediterranean, J. Geophys. Res., 105, 4399–4407, 2000.

Lamarque, J.-F., Hess, P. G., Emmons, L., Buja, L., Washington, W., and Granier, C.: Tropospheric ozone evolution between 1890 and 1990, J. Geophys. Res., 110, D08304, doi: 10.1029/2004JD005537, 2005.

Lelieveld, J., Berresheim, H., Borrmann, S., Crutzen, P. J., Dentener, F. J., Fischer, H., Feichter, J., Flatau, P. J., Heland, J., Holzinger, R., Korrmann, R., Lawrence, M. G., Levin, Z., Markowicz,

K. M., Mihalopoulos, N., Minikin, A., Ramanathan, V., de Reus, M., Roelofs, G. J., Scheeren, H. A., Sciare, J., Schlager, H., Schultz, M., Siegmund, P., Steil, B., Stephanou, E. G., Stier, P., Traub, M.,Warneke, C.,Williams, J., and Ziereis, H.: Global air pollution crossroads over the mediterranean, Science, 298, 794–799, doi:10.1126/science.1075457, 2002.

Liu, J., Jones, D. B. A., Zhang, S., and Kar, J.: Influence of interannual variations in transport on summertime abundances of ozone over the Middle East, J. Geophys. Res., 116, D20310, doi:10.1029/2011JD016188, 2011.

Ma, J., Zhou, X., and Hauglustaine, D.: Summertime tropospheric ozone over China simulated with a regional chemical transport model, Part 2. Source contribution and budget, J. Geophys. Res., 107 (D22), 4612, doi:10.1029/2001JD001355, 2002.

Papayannis, A., Balis, D., Zanis, P., Galani, E., Wernli, H., Zerefos, C., Stohl, A., Eckhardt, S., and Amiridis, V.: Sampling of an STT event over the Eastern Mediterranean region by lidar and electrochemical sonde, Ann. Geophys., 23, 2039–2050, doi:10.5194/angeo-23-2039-2005, 2005.

Pfister, G., Emmons, L. K., Hess, P. G., Honrath, R., Lamarque, J.-F., Val Martin, M., Owen, R. C., Avery, M., Browell, E. V., Holloway, J. S., Nedelec, P., Purvis, R., Rywerson, T. B., Sachse, G. W., and Schlager, H.: Ozone production from the 2004 North American boreal fires, J. Geophys. Res., 111, D24S07, doi:10.1029/2006JD007 695, 2006.

Pfister, G. G., Emmons, L. K., Hess, P. G., Lamarque, J.-F., Thompson, A. M., and Yorks, J. E.: Analysis of the summer 2004 ozone budget over the United States using Intercontinental Transport Experiment Ozonesonde Network Study (IONS) observations and Model of Ozone and Related Tracers (MOZART-4) simulations, J. Geophys. Res., 113, D23306, doi:10.1029/2008JD010190, 2008.

Pfister, G. G., Walters, S., Emmons, L. K., Edwards, D. P., and Avise, J.: Quantifying the contribution of inflow on surface ozone over California during summer 2008, J. Geophys. Res. Atmos., 118, 12,282–12,299, doi:10.1002/2013JD020336, 2013.

R'Honi, Y., Clarisse, L., Clerbaux, C., Hurtmans, D., Duflot, V., Turquety, S., Ngadi, Y., and Coheur, P.-F.: Exceptional emissions of NH_3 and HCOOH in the 2010 Russian wildfires, Atmos. Chem. Phys., 13, 4171-4181, doi:10.5194/acp-13-4171-2013, 2013.

Richards, N. A. D., Arnold, S. R., Chipperfield, M. P., Miles, G., Rap, A., Siddans, R., Monks, S. A., and Hollaway, M. J.: The Mediterranean summertime ozone maximum: global emission sensitivities and radiative impacts, Atmos. Chem. Phys., 13, 2331-2345, doi:10.5194/acp-13-2331-2013, 2013.

Rodwell, M. J. and Hoskins, B. J.: Monsoons and the dynamics of deserts, Q. J. R. Meteorol. Soc., 122, 1385–1404, doi:10.1002/qj.49712253408, 1996.

Rodwell, M. J. and Hoskins, B. J.: Subtropical anticyclones and summer monsoons, J. Climate, 14, 3192–3211, 2001

Roelofs, G. J., Scheeren, H. A., Heland, J., Ziereis, H., and Lelieveld, J.: A model study of ozone in the eastern Mediterranean free troposphere during MINOS (August 2001), Atmos. Chem. Phys., 3, 1199–1210, doi:10.5194/acp-3-1199-2003, 2003.

Safieddine S., Clerbaux C., George M., Hadji-Lazaro J., Hurtmans D., Coheur P.-F., Wespes C., Loyola D., Valks P., Hao N.: Tropospheric ozone and nitrogen dioxide measurements in urban and rural regions as seen by IASI and GOME-2, J. Geo. Phys. Res : Atmospheres 118, 18, 10555-10566, 2013.

Schubert, S., Wang, H., and Suarez, M.: Warm season sub-seasonal variability and climate extremes in the Northern Hemisphere: the role of stationary Rossby waves. J. Climate, 24, 4773-4792, 2011.

Sprenger, M. and Wernli, H.: A northern hemispheric climatology of cross-tropopause exchange for the ERA15 time period 1979–1993), J. Geophys. Res., 108, 8521, doi:10.1029/2002JD002636, 2003.

Stohl, A., Spichtinger-Rakowsky, N., Bonasoni, P., Feldmann, H., Memmesheimer, M., Scheel, H. E., Trickl, T., Hubener, S. H., Ringer, W., and Mandl, M.: The influence of stratospheric intrusions on alpine ozone concentrations, Atmos. Environ., 34,1323–1354, 2000.

Tuccella, P., Curci, G., Visconti, G., Bessagnet, B., Menut, L., and Park, R. J.: Modeling of gas and aerosol with WRF/Chem over Europe: Evaluation and sensitivity study, J. Geophys. Res., 117, D03303, doi:10.1029/2011JD016302, 2012.

Turquety, S., Hurtmans, D., Hadji-Lazaro, J., Coheur, P.-F., Clerbaux, C., Josset, D., and Tsamalis, C.: Tracking the emission and transport of pollution from wildfires using the IASI CO retrievals: analysis of the summer 2007 Greek fires, Atmos. Chem. Phys., 9, 4897–4913, 2009, http://www.atmos-chem-phys.net/9/4897/2009/.

Tyrlis, E., Lelieveld, J., and Steil, B.: The summer circulation in the eastern Mediterranean and the Middle East: influence of the South Asian Monsoon, Clim. Dynam., 40, 1103–1123, doi:10.1007/s00382-012-1528-4, 2013a.

Wespes, C., Emmons, L., Edwards, D. P., Hannigan, J., Hurtmans, D., Saunois, M., Coheur, P.-F., Clerbaux, C., Coffey, M. T., Batchelor, R. L., Lindenmaier, R., Strong, K., Weinheimer, A. J., Nowak, J. B., Ryerson, T. B., Crounse, J. D., and Wennberg, P. O.: Analysis of ozone and nitric acid in spring and summer Arctic pollution using aircraft, ground-based, satellite observations and MOZART-4 model: source attribution and partitioning, Atmos. Chem. Phys., 12, 237-259, doi:10.5194/acp-12-237-2012, 2012.

Wiedinmyer, C., Akagi, S. K., Yokelson, R. J., Emmons, L. K., Al-Saadi, J. A., Orlando, J. J., and Soja, A. J.: The Fire Inventory from NCAR (FINN) – a high resolution global model to estimate the emissions from open burning, Geosci. Model Dev., 4, 625–641, 2011.

Zanis, P., Hadjinicolaou, P., Pozzer, A., Tyrlis, E., Dafka, S., Mihalopoulos, N., and Lelieveld, J.: Summertime free-tropospheric ozone pool over the eastern Mediterranean/Middle East, Atmos. Chem. Phys., 14, 115-132, doi:10.5194/acp-14-115-2014, 2014.

Zbinden, R. M., Thouret, V., Ricaud, P., Carminati, F., Cammas, J.-P., and Nédélec, P.: Climatology of pure tropospheric profiles and column contents of ozone and carbon monoxide using MOZAIC in the mid-northern latitudes (24° N to 50° N) from 1994 to 2009, Atmos. Chem. Phys., 13, 12363-12388, doi:10.5194/acp-13-12363-2013, 2013.

Ziv, B., Saaroni, H., and Alpert, P.: The factors governing the summer regime of the Eastern Mediterranean, Int. J. Climatol., 24, 1859–1871, 2004

Table 1: List of geographic location of the EMEP O_3 monitoring ground stations used in this study, with the corresponding altitude above mean sea level.

Code	Station name	Latitude (°N)	Longitude (°E)	Altitude (m)
CY02	Ayia Marina	35.04	33.06	532
ES06	Mahón	39.87	4.32	78
ES07	Víznar	37.30	-3.53	1265
ES10	Cabo de Creus	42.32	3.32	23
ES12	Zarra	39.08	-1.10	885
ES14	Els Torms	41.39	0.73	470
GR02	Finokalia	35.31	25.66	250
MK07	Lazaropole	41.32	20.42	1332

Table 2. Pearson correlation coefficient, bias and the corresponding mean normalized bias (MNB) of each EMEP and WRF-Chem ground station data localized in Fig. 2, for the period JJA 2010.

Station name	Corr. Coef. With WRF-Chem	Bias (ppbv)	MNB (%)
CY02	0.63	-7.78	(-14.2%)
ES06	0.41	+7.26	(+20.9%)
ES07	0.77	-7.24	(-13.4%)
ES10	0.72	+1.43	(+3.6%)
ES12	0.80	-5.96	(-12.7%)
ES14	0.78	-2.99	(-6.4%)
GR02	0.62	-7.38	(-11.3%)
MK07	0.57	-16.65	(-23.9%)

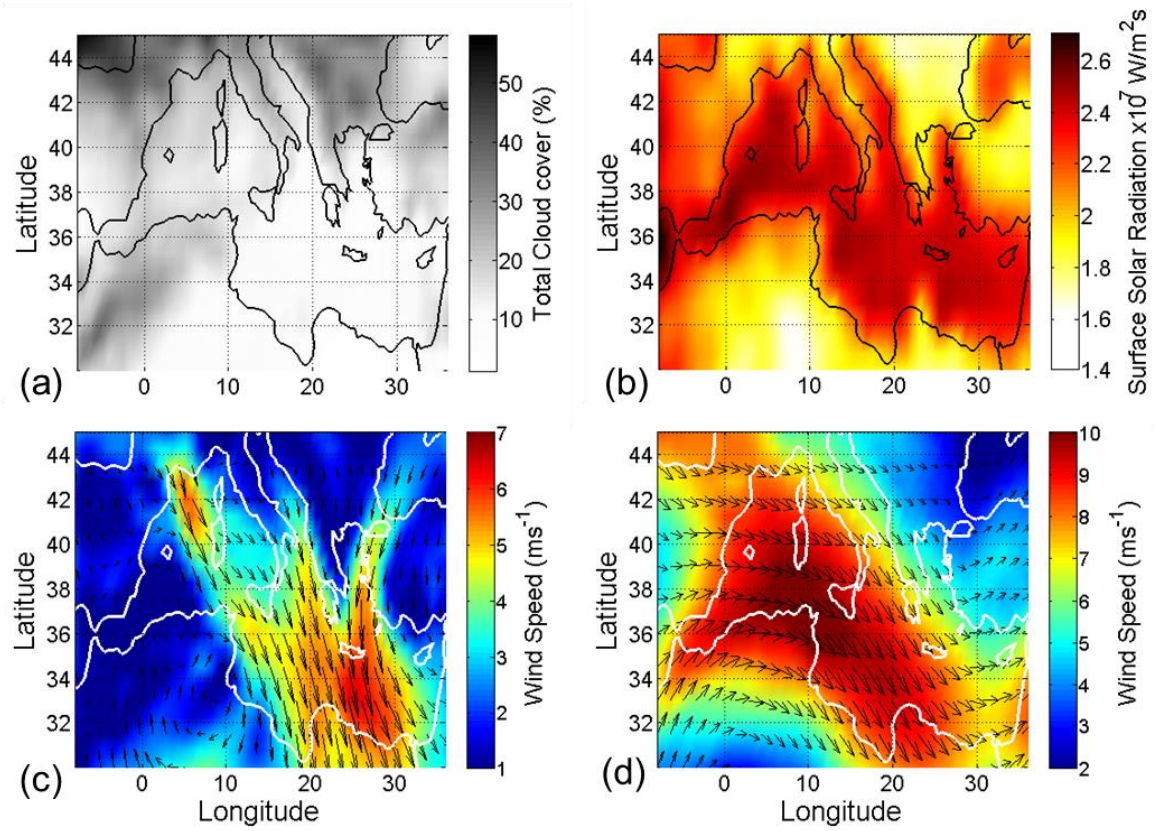

1351

1352 **Fig.1.** An example of the ECMWF (European Centre for Medium-Range Weather Forecasts)
1353 Reanalysis (ERA-Interim) for the period June-July-August (JJA) 2010 for: (a) total cloud
1354 coverage, (b) 12:00 UTC solar radiation reaching the surface and (c) wind speed and direction
1355 averaged from the surface to 750 hPa and (d) wind speed and direction averaged from 750 to 400
1356 hPa.

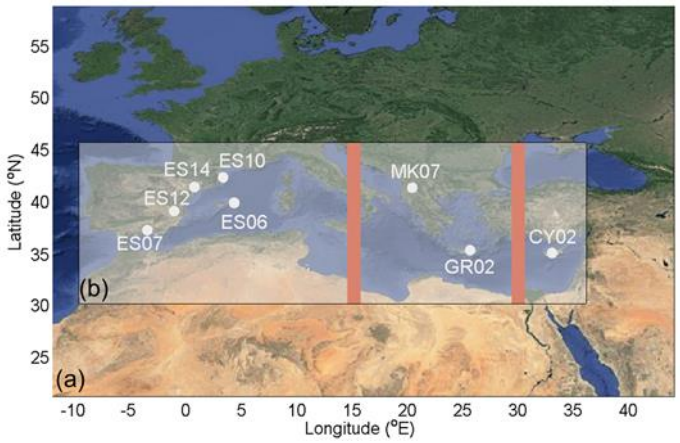

1357

Fig. 2. (a) The enlarged WRF-Chem model run domain. (b) IASI and WRF-Chem domain used in this study. White dots correspond to the location of the EMEP ground stations and the orange strips correspond to the longitudinal transects used in Figures 5 and 10.

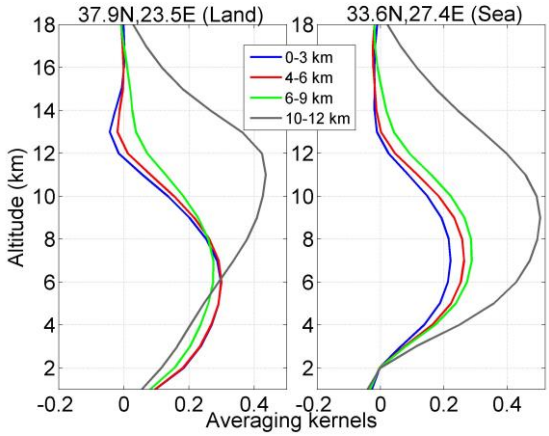

Fig. 3. Random O_3 averaging kernels over the Mediterranean: the functions are for the [surface-3], [4-6], [6-9], and [10-12] km partial columns characterizing a retrieval for an observation chosen randomly above land (Greece, left panel) and above the sea (right panel) during June 2010.

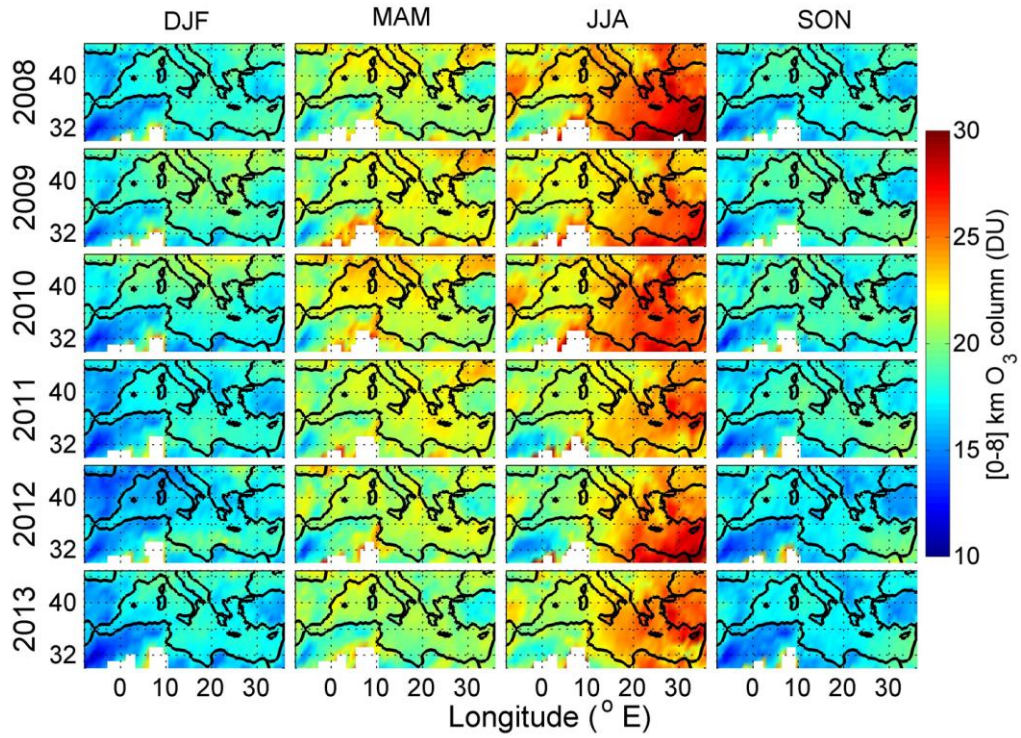

Fig. 4. Six years seasonal variation of [0-8] km integrated IASI O_3 column over the Mediterranean region for winter, spring, summer and autumn. White pixels correspond to a filter applied on poor spectral fits, because of emissivity issues in the FORLI radiative transfer above the Sahara desert.

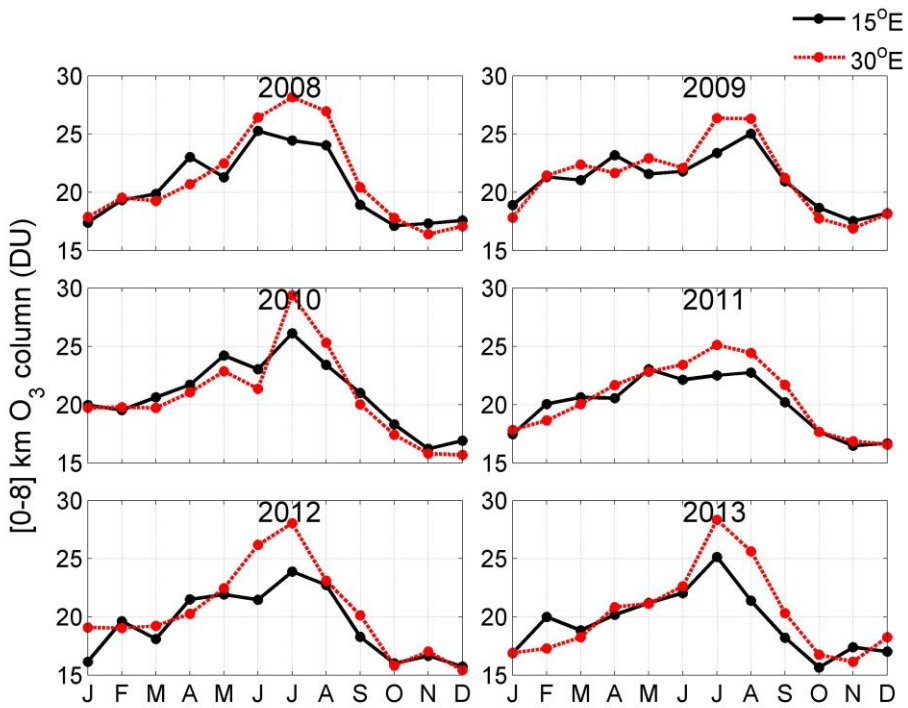

Fig. 5. Six years monthly variation of the integrated [0-8] km IASI O_3 column averaged over [30°N-45°N] at 15°E (in black) and 30°E (in red). Higher summer values are observed to the east of the basin at 30°E.

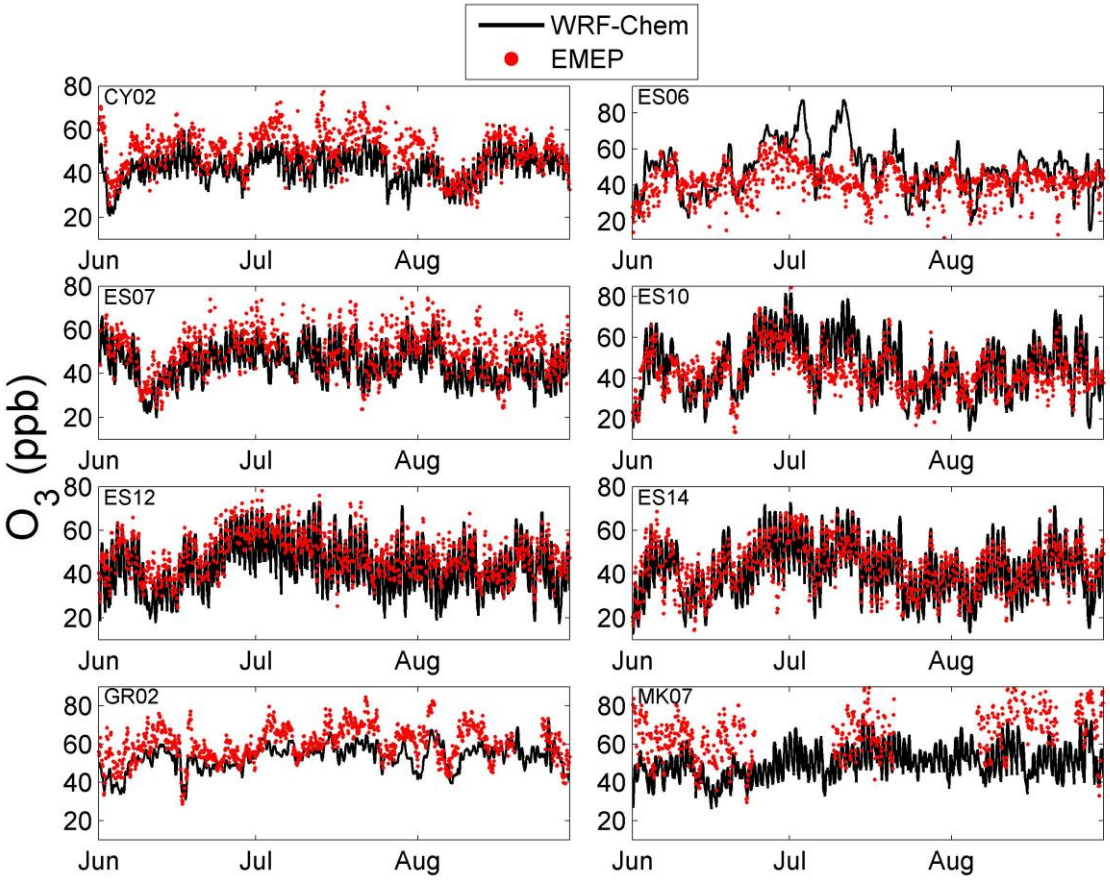

Fig. 6. O_3 time series of EMEP and WRF-Chem data at the surface for the stations localized in Fig. 2, for the period JJA 2010.

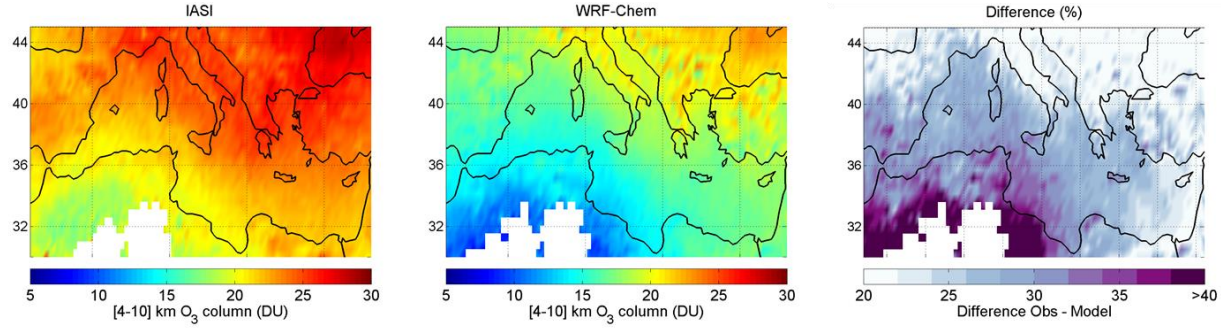

Fig. 7. Average [4-10] km O_3 column for JJA 2010 from IASI and WRF-Chem and their relative difference (%). White pixels correspond to a filter applied to poor spectral fits above the Sahara desert.

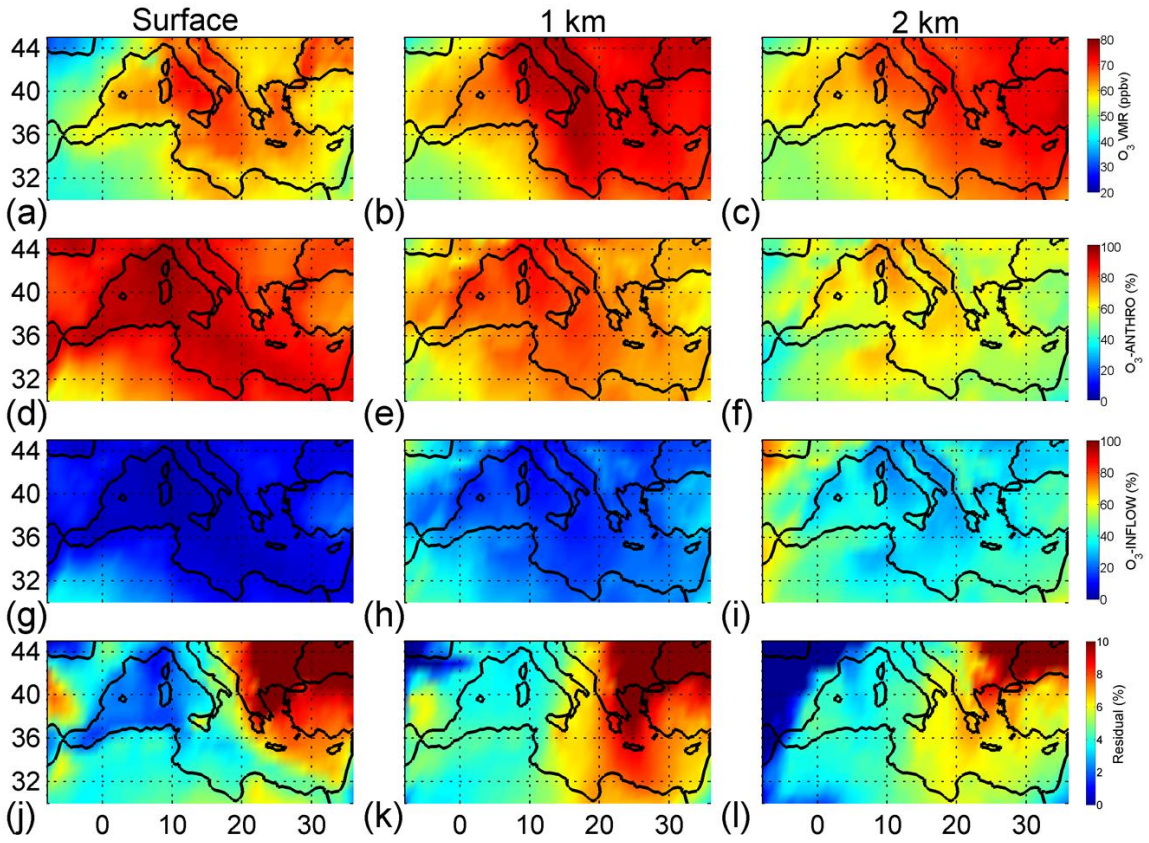

Fig. 8. WRF-Chem spatial distributions of (a-c) O_3 mixing ratios (ppbv), (d-f) O_3 anthropogenic tracer relative contributions (%), (g-i) O_3 inflow tracer relative contribution, and (j-l) the residual (100%-($O_{3\text{-ANTHRO}}$%+$O_{3\text{-INFLOW}}$%)) averaged over the period JJA 2010 at the surface, 1 km and 2 km. Note that the colorbar for the residual plots is different.

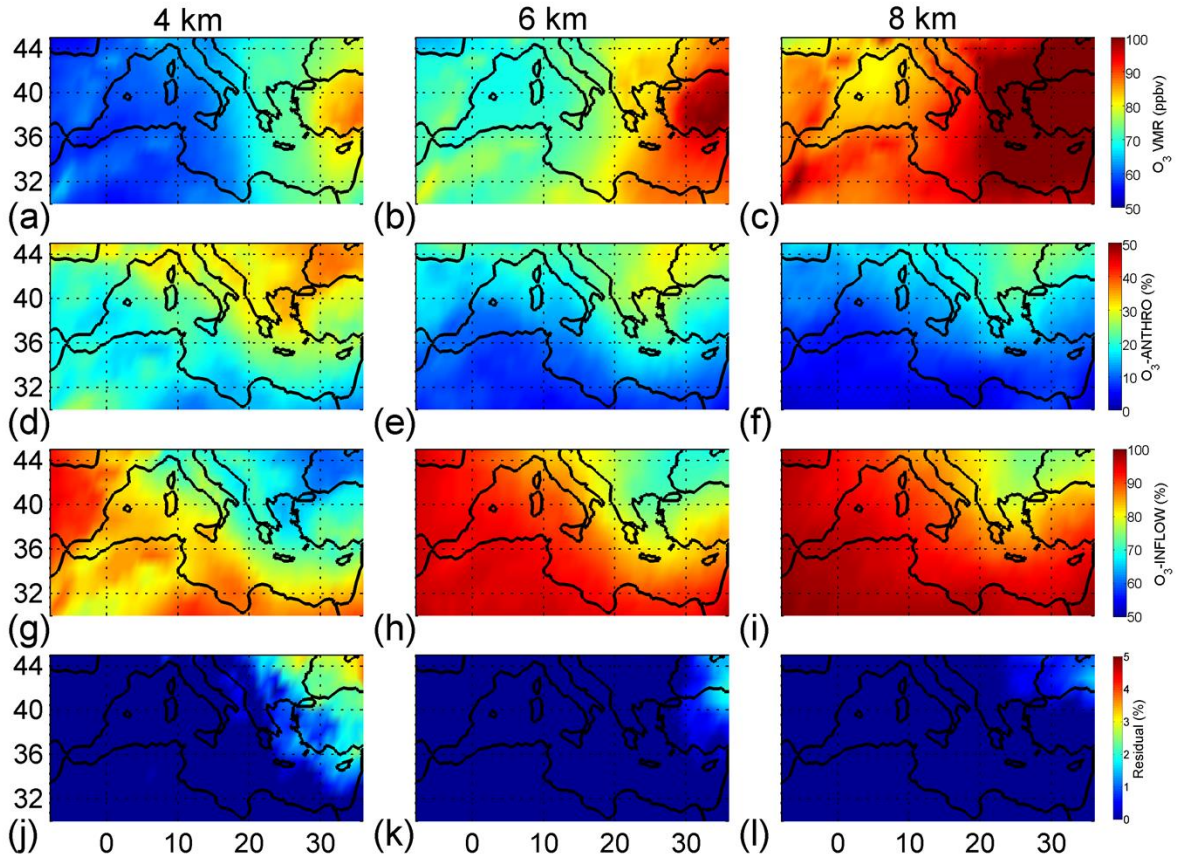

Fig. 9. Same as Fig. 8 but for 4, 6 and 8 km.

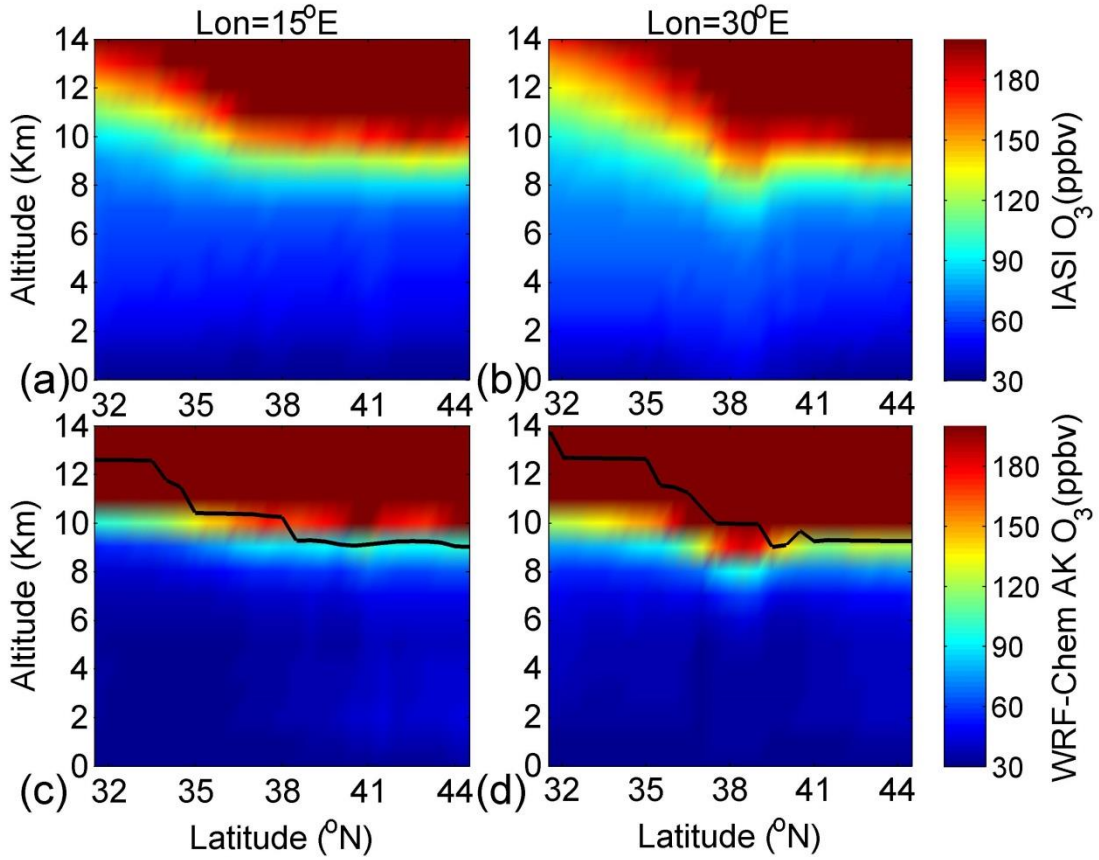

Fig.10. Mean latitude-altitude cross sections of IASI-O_3 (a-b) and modeled-O_3 (c-d) averaged over JJA 2010 at 15°E (left) and 30°E (right). Black line corresponds to the dynamical tropopause height.

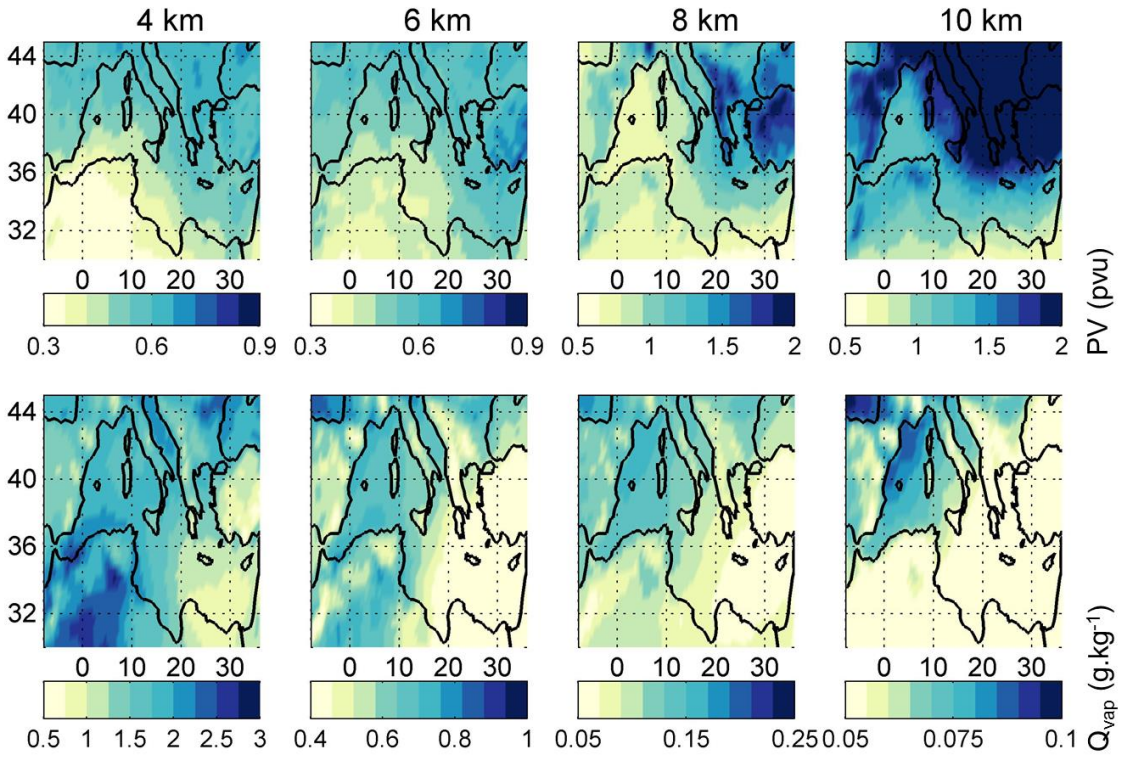

Fig. 11. WRF-Chem (a) potential vorticity (PV) at 4, 6, 8 and 10 km over the Mediterranean region for JJA 2010 and (b) water vapor mixing ratio (Q_{vap}) for the same vertical levels and time period.